

Human-like generalization in a machine through predicate learning

Leonidas A. A. Doumas^{1*},
Guillermo Puebla¹,
Andrea E. Martin²

¹School of Philosophy, Psychology, and Language Sciences, The University of Edinburgh

²Max Planck Institute for Psycholinguistics, Nijmegen, The Netherlands

*Address for correspondence: 7 George Square, Edinburgh, EH8 9JZ, UK; email:
alex.doumas@ed.ac.uk

Abstract

Humans readily generalize, applying prior knowledge to novel situations and stimuli. Advances in machine learning and artificial intelligence have begun to approximate and even surpass human performance, but machine systems reliably struggle to generalize information to untrained situations. We describe a neural network model that is trained to play one video game (Breakout) and demonstrates one-shot generalization to a new game (Pong). The model generalizes by learning representations that are functionally and formally symbolic from training data, without feedback, and without requiring that structured representations be specified a priori. The model uses unsupervised comparison to discover which characteristics of the input are invariant, and to learn relational predicates; it then applies these predicates to arguments in a symbolic fashion, using oscillatory regularities in network firing to dynamically bind predicates to arguments. We argue that models of human cognition must account for far-reaching and flexible generalization, and that in order to do so, models must be able to discover symbolic representations from unstructured data, a process we call *predicate learning*. Only then can models begin to adequately explain where human-like representations come from, why human cognition is the way it is, and why it continues to differ from machine intelligence in crucial ways.

KEYWORDS: predicate learning, generalization, neural networks, symbolic-connectionism, video games

People use what they already know to solve new problems. In domain from sports, music, language, mathematics, or gaming, people learn from their environment, refine what they know from experience, and employ strategies they learned in one context in another. Despite its importance for how humans learn, however, the ability to generalize across contexts presents a striking lacuna for machine learning systems.

Recent advances in machine learning (e.g., LeCun, Bengio, & Hinton, 2015) have produced deep neural network (DNN) systems that reach and even exceed human levels of performance on a range of cognitive tasks. For example, recent DNNs learned to master an impressive number of Atari games (Mnih et al., 2015). DNNs are general, in that they can learn to perform a variety of tasks without *a priori* background knowledge. Nevertheless, while DNNs readily perform *interpolation* (i.e., generalization to untrained items from within the bounds of the training set), they struggle to perform *extrapolation* (i.e., generalization to items from outside the bounds of the training set). While a human learner who plays one video game, like Breakout, will quickly generalize to playing a new game, like Pong, in stark contrast, DNNs trained to play one game must be retrained in order to play any additional games (Mnih et al., 2015).

That DNNs have difficulty extrapolating their knowledge is well known and appears to stem from their explicit lack of structured (i.e., compositional or symbolic) representations (Forbus et al., 2017; Lake, Ullman, Tenenbaum, & Gershman, 2017; Marcus, 1998, 2018a). By contrast, accounts of how humans generalize are frequently based on powerful symbolic languages that include structured relations (or predicates), which can be promiscuously applied to new arguments (Anderson, 2008; Hummel & Holyoak, 1997, 2003; Tenenbaum, Kemp, Griffiths, & Goodman, 2011). Structured representations allow the flexible transfer of information across contexts because the same representations can be used to characterize very different situations (Figure 1). For example, one recent model of hand-writing recognition (Lake et al., 2015) can learn to recognize and even recreate novel hand-written characters after only a single exposure, because it represents those characters in terms of predicates, *attached-at-start(x,y)*, *attached-along(x,y)*, and *attached-at-end(x,y)*, that relate possible line segments together. However, models that exploit structured representations face a challenge that is complementary to that which DNNs face: They characteristically require the modeler to specify a collection of necessary representational structures in advance of any actual learning (Hummel & Holyoak, 1997, 2003; Kemp, 2015; Lake et al., 2015; Tenenbaum, Kemp, Griffiths, & Goodman, 2011). So, while structure-based models generalize more flexibly than DNNs, they do not possess the same capabilities to learn from scratch.

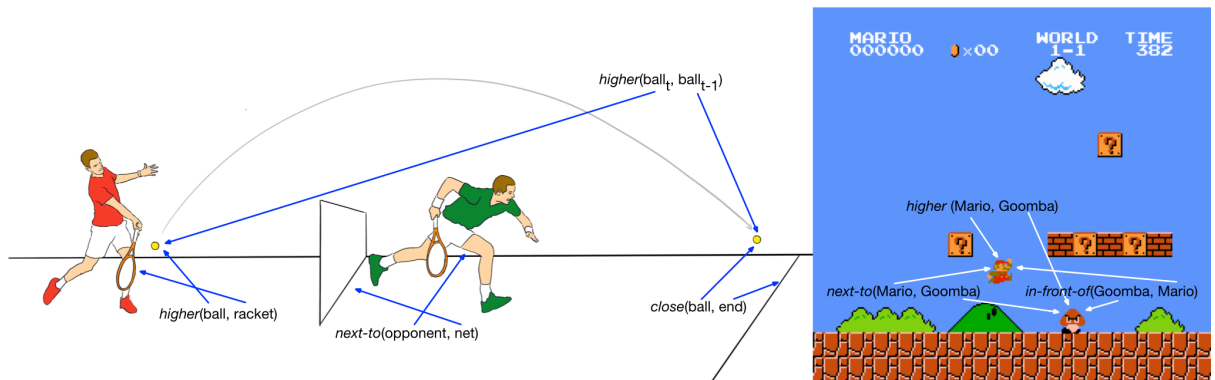


Figure 1. Representations of relations and predicates in two disparate domains: video games and tennis. Many of the same relations that support reasoning about a strategic shot in tennis allow also support

reasoning about a strategic move in a game of Super Mario Bros. (e.g., the *higher* relation comes into play when planning a drop shot in tennis, or a jump attack by Mario).

We describe a neural network model that bridges the gap between these frameworks, a general learner that discovers powerful symbolic representations from experience. The model is trained via a process that we call *predicate learning*, and the representations that it learns allow it to reach human-level performance on some tasks, and, crucially, to generalize and transfer that expertise in a human-like fashion, quickly (in a single shot) and without explicit feedback. The architecture, called DORA (*Discovery of Relations by Analogy*; see also Doumas, Hummel, & Sandhofer, 2008), is based on two influential ideas from cognitive science and neuroscience. First, learning and generalization depend upon a process of comparison (e.g., Gentner, 2003; Holyoak & Thagard, 1996). Second, information in neural computing systems can be carried by the oscillatory regularities that emerge as its component units fire (e.g., Buzsáki, 2006, von der Malsburg, 1986, 1995). In brief, DORA uses unsupervised comparison to discover which characteristics of the input are invariant, and to learn functional predicates; it then applies these predicates to arguments in a symbolic fashion, using oscillatory regularities to dynamically bind predicates and arguments. DORA learns representations that are functionally and formally symbolic from training data, without feedback, and without requiring that structured representations be specified a priori. We demonstrate that these capacities allow DORA to successfully master a video game with minimal prior knowledge, just like a DNN, but that DORA can then transfer its expertise in that game to a new game in one shot, extrapolating its knowledge in a manner that closely resembles human players.

Learning structured representations

DORA is descended from of the symbolic-connectionist system LISA (Hummel & Holyoak, 1997, 2003). DORA learns to represent structured (i.e., functionally symbolic) representations from examples without feedback. DORA is a neural network model, with banks of layered units that are connected to a common pool of feature units. Activation flows from the current focus bank (the current attentional state of the model) to other banks (active memory and long-term memory (LTM)) via these shared feature units. DORA can learn mapping connections between corresponding coactive units across banks using a modified Hebbian learning algorithm (Doumas et al., 2008; Hummel & Holyoak, 1997). Full details of the model's operation appear in S1. Source code is available online (see Acknowledgements).

In order to learn a symbolic relational representation, a system must solve four problems:

Problem 1: Learn to respond to relevant invariance (e.g., similarity and relative magnitude; Figure 2A). DORA solves this problem by exploiting the property that absolute magnitude information for spatial dimensions is encoded in an analog fashion by neural systems (Engel et al., 1996; Furmanski & Engel, 2000; Moore & Engel, 2001). When two objects, O_i and O_j , that differ in value on some magnitude dimension (e.g., size) are co-activated (Figure 2A,i), and the units coding O_i and O_j compete to stay active (via lateral inhibition; Figure 2A,ii). The object with the larger dimensional value will win the competition and become active first (as it is coded by a greater extent of units; Figure 2A,iii), while the lesser object will lose and become active next (Figure 2A,iv). By contrast, when two items of the same magnitude are compared, they will settle into a state of mutual co-activation. DORA exploits these invariant emergent patterns by learning specific responses to them. DORA learns to activate a unit (or set of units) in response to winning the competition (the invariant for “moreness”), another unit (or set of units) in response to losing the competition (the invariant for “lessness”), and another unit (or

set of units) in response to mutually co-activation (the invariant for “sameness”), and learns connections between these units and any active object units via Hebbian learning (Figure 2A,iii-iv). Details of learning this circuit in S2.

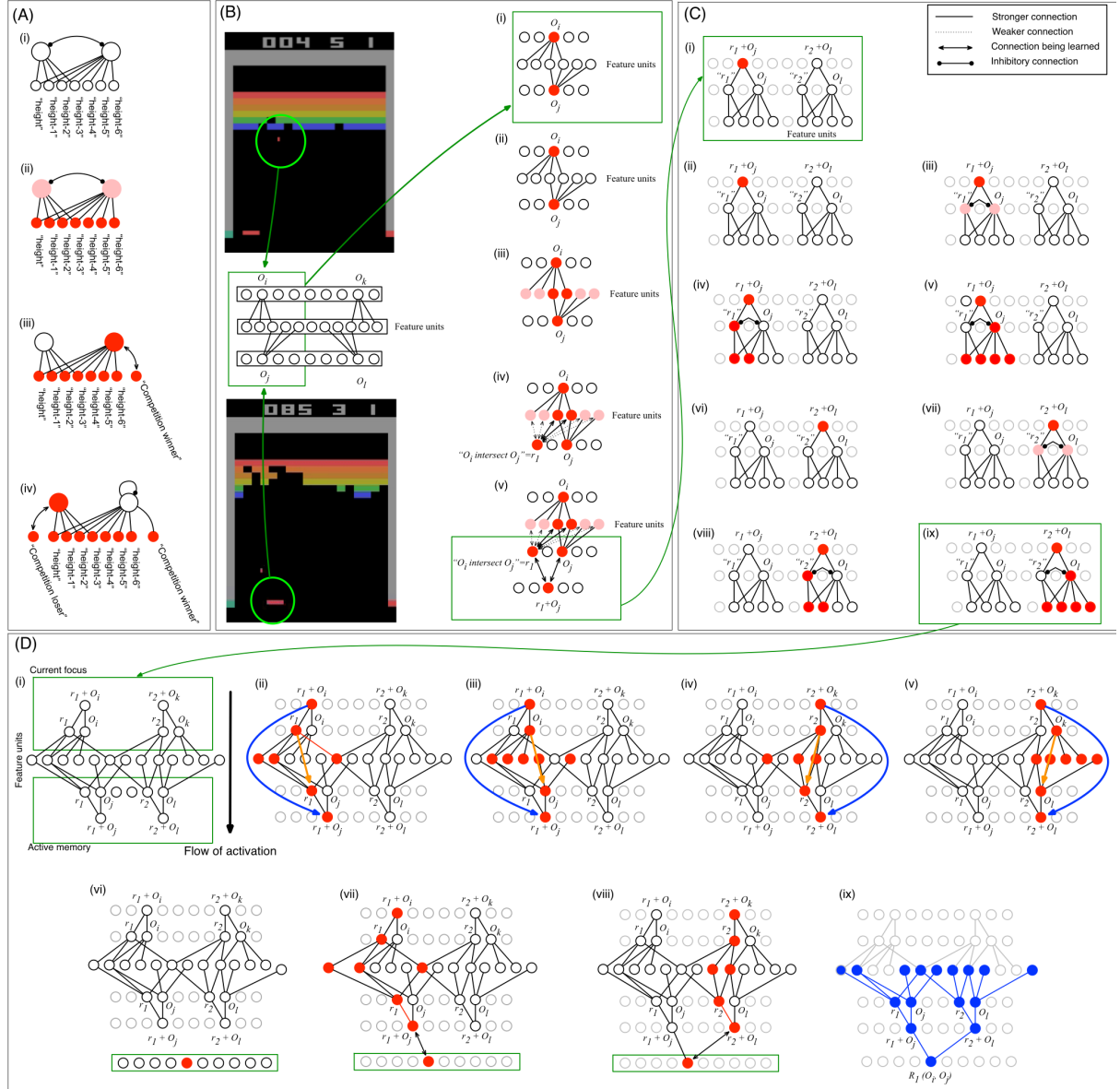


Fig. 2. Learning in DORA. (A) Invariant responses to similarity and relative magnitude emerge when objects with absolute magnitudes are compared. (i) Two representations of objects (large circles) with different values on some dimension are compared. (ii) Magnitude representations are activated, and the objects compete, via lateral inhibition, to become active (red = more active unit). (iii). The object with the greater magnitude wins the competition—the invariant signal for greater magnitude—and learns a connection to a node indicating the competition winner. (iv) The object with the lesser magnitude becomes active next—the invariant signal for lesser magnitude—and learns a connection to a node indicating the competition loser. (B) Isolation and explicit representation of invariant properties via comparison. (i) Two objects, O_i and O_j , are compared (co-activated). (ii) Objects pass activation to their constituent features. (iii) Shared features receive roughly twice as much input and become roughly twice as active as unshared features. (iv) A recruited unit, r_l , learns connections to the active features in proportion to their activation (via Hebbian learning). Unit r_l explicitly codes for the intersection of O_i and O_j . (v) A unit at another layer of the network learns connections to the active units O_j and r_l , coding their conjunction. (C) Learned representations are dynamically bound to arguments by systematic phase-lag. (i) The pair $r_l + O_j$ learned in (B), and another pair, $r_2 + O_l$ learned as in (B). (ii) Unit coding for $r_l + O_j$ conjunction becomes active, and (iii) passes activation to the r_l and O_j units, which compete, via lateral inhibition, to become active. (iv) r_l becomes active first. (v) O_j become active next. The direct sequence of firing marks the binding of r_l to O_j . (vi-ix) A similar pattern emerges when the $r_2 + O_l$ role-binding becomes active. (D) Lower arity

representations are conjoined into multi-place relational structures. (i) Role-filler pairs $r1+Oj$ and $r2+Ol$ from (C) are compared to role-filler pairs $r1+Oi$ and $r2+Ok$. (ii) As a result of phase-lag binding in (C), bound role-filler pairs will oscillate. Units coding for $r1$ in the focus of attention become active. Activation flows from the focus of attention to active memory via the shared feature units activating units coding for $r1$ in active memory (indicated by orange and blue arrows). (iii) Next, the units coding for Oj and Ol similarly become active. (iv) Units coding for $r2$ become active, (v) followed by the units coding for their arguments. (vi) A unit at another layer of the network is recruited and learns connections to role-filler pairs as they become active—(vii) the $r1+Oj$ pair, (viii) then the $r2+Ol$ pair. (ix) The result is a structure (nodes coloured blue) that functions as a multi-place predicate.

Problem 2: Isolate and explicitly represent invariant perceptual features or properties (Figure 2B). Comparing (and co-activating) distributed representations of items, O_i and O_j , naturally reveals shared and unshared features of the two items. Specifically, features shared by O_i and O_j will receive roughly twice as much input and, therefore, become roughly twice as active as unshared features (Figure 2B,iii). DORA exploits this emergent regularity by learning connections between a recruited unit, r_l , and active feature units by Hebbian learning (Figure 2B,iv). The result is a unit explicitly encoding the intersection of the compared items, and a solution to the isolation problem. In addition, a unit at another layer of the network learns connections to r_l and O_j (Figure 2B,v), conjunctively coding a link between them.

Problem 3: Dynamically bind learned representations to arguments (Figure 2C). DORA dynamically binds representations learned by comparison to arguments, producing functional single-place predicates. When laterally inhibitive units are linked by a conjunctive node, they will naturally oscillate out of synchrony and in direct sequence (phase-lag-1) when the conjunctive unit becomes active (Figure 2C,i-v). DORA exploits this emergent oscillatory pattern as a binding signal. Specifically, bound units fire in direct sequence, and systematically out of synchrony with other bound pairs (Figure 2C,vi-ix). In short, identity information is carried by *what* units are active, and binding information is carried by *when* those units are active. This binding signal is dynamic in that the same units are used to represent complementary bindings through different firing orders (e.g., binding r_1 to object O_j and r_2 to object O_i , amounts to the units coding for r_1 firing, followed by the units for O_j , and then the units coding for r_2 firing, followed by the units coding for O_i). As we demonstrate below the resulting representations are functional predicate-object, or role-filler, pairs.

Problem 4: Combine lower arity representations into multi-place relational structures (Figure 2D). When DORA compares and aligns two structurally similar sets of bound elements (Figure 2D,i), the aligned (or corresponding) units across the two sets will oscillate systematically (Figure 2D,ii-v). This pattern only emerges in the model only when role-filler pairs are already linked into a whole relational structure, or when multiple similar co-occurring role-filler pairs are compared. Thus, the pattern is a reliable signal that DORA exploits to learn multi-place relational structures. As the pattern emerges, DORA learns connections between a unit at a higher layer of the network and active conjunctive nodes by Hebbian learning (Figure 2D,vi-viii). The resulting representation (Figure 2D,ix) is a functionally symbolic multi-place relational predicate. At the layer of feature units, objects, properties, and roles are coded in a distributed fashion. At the next later, collections of properties are conjunctively coded as tokens of individual objects and predicates. At the next layer, role-filler pairs are conjunctively bound. At the top layer, conjunctively coded role-filler pairs are themselves conjunctively coded into whole multi-place relations. The resulting structure allows for storage in LTM, and when the representation becomes active, dynamic binding information is carried in the temporal patterns of firing that emerge, with tokens for individual predicates and objects bound by their firing phase-lag (Figure 2C).

Results

Humans (two Breakout and Pong novices), DORA, and two neural networks, a deep-Q-network (DQN; Mnih et al., 2015), and a deep neural network (DNN; LeCun, Bengio, & Hinton, 2015) were compared for their ability to make far-reaching generalizations. Specifically, we trained these models to play one videogame (Breakout), and then tested their ability to generalize to a different videogame (Pong) without any explicit training. Finally, we evaluated these systems' ability to switch back to playing the original game, after time spent learning to play the second.¹ See S3 for details of all simulations.

For the first 250 games of Breakout, DORA made random moves, generating game states from which it learned structured representations in an unsupervised manner as described above (see S3 for details). DORA successfully learned predicate representations of relations such as *higher* (or *moreY* (object1, object2)), and *right-of* (or *moreX* (object1, object2)). As demonstrated below, the representations it learned are symbolic, and support extrapolatory generalization outside the training situation (additional tests are reported in S3). DORA then attempted to learn to play Breakout using simple supervised learning (e.g., Agrawal et al., 1993). DORA used the representations that it had learned previously to represent the current game screen and then made a response. Associations between representational states and successful moves were reinforced. While much more sophisticated methods for model selection exist, we employed this very simple solution as a proof of concept.

The DQN was trained using deep Q-learning with fixed frame skipping during learning (Mnih et al., 2015). Atari game emulation often includes random frame skipping (partially to emulate the jerky nature of the game system). As such, we also included a DNN trained in a supervised manner with the backpropagation algorithm, but using random frame skipping. For comparison, we also trained two versions of DORA, one with random frame skipping (rDORA) and one with fixed frame skipping (fDORA).

Figure 3A shows the performance of all networks on Breakout as an average score of the last 100 games played (after reaching plateauing performance), and a high score. Unsurprisingly, the networks without random frame skipping (DQN and fDORA) performed much better than those with random frame skipping. However, the DNN and rDORA also learned to perform well, matching and surpassing the baseline of a human player, respectively.

¹ While we discuss the generalization in terms of learning to play Breakout and generalizing to playing Pong, the results were the same when training moved in the opposite direction (i.e., training on Pong and generalizing to Breakout).

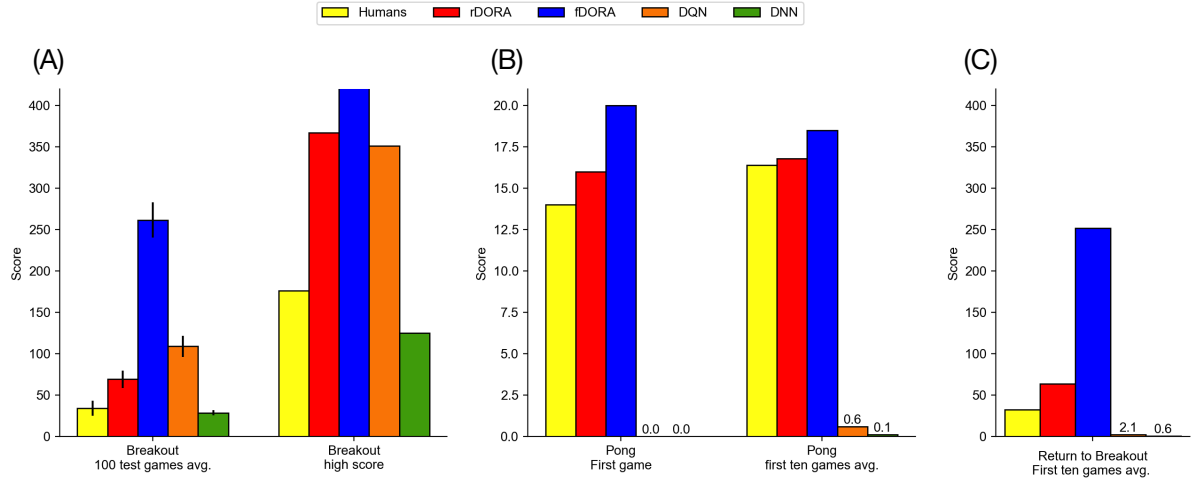


Figure 3. Results of game play simulations with Humans, DORA, DQN and DRNN. (a) Performance of rDORA, fDORA, the DQN and the DRNN on Breakout as an average and high score. (b) Results of humans and networks playing Pong after training on Breakout. (c) Results of humans and networks when returning to play Breakout after play or learning to play Pong.

We then tested the capacity of the networks to play a new videogame, Pong. DORA had learned to play Breakout by learning associations between relational configurations and actions. Because DORA’s representations of these relational configurations are symbolic, they apply readily to untrained situations. That is, the predicates DORA uses to describe a relational configuration in Breakout can apply—or be bound to—items in any other situation (including novel situations). During its first game of Pong, DORA represented the game state using the relations it had learned playing Breakout and discovered the correspondence between the action sets in the two games: particularly, *moreY/lessY* of the paddle (the paddle moves up and down across the Y dimension) in Pong and *moreX/lessX* of the paddle (the paddle moves left and right across the X dimension) in Breakout. This correspondence allowed DORA to infer via relational generalization (Doumas et al., 2008; Hummel & Holyoak, 2003; S1 and S4 for details) the relational configurations that predict specific moves in Pong, using its knowledge of the relational configurations that predict specific moves from Breakout. For example, just as *moreX* (ball, paddle) predicted a *moreX* move of the paddle in Breakout, *moreY* (ball, paddle) predicts a *moreY* move of the paddle in Pong.

Figure 3B shows the performance of a human player and the networks on the first game of Pong after training on Breakout and the average performance over the first 10 games playing Pong. Like a human player, DORA performed at a high level on Pong on a single exposure to the game, and, like humans, DORA played Pong at a high level. By contrast, the DQN and DNN show poor performance—which is unsurprising given previous results using DNNs and transferring to different contexts (as noted above; Mnih et al., 2015, Marcus, 2018a).

Finally, we trained the DQN and DNN on Pong. We then tested the capacity of the networks to return to playing Breakout. Figure 3C shows the performance of a human player and the networks on the first game returning to play Breakout. Like a human player, DORA returns to playing the original game with little difficulty. By contrast, the DQN and DRNN, show poor performance, indicating that learning to play a new game interferes with the capacity to play old games.²

² While recent advances such as (Kirkpatrick et al., 2017) have shown how such catastrophic forgetting can be avoided in neural networks, importantly, these systems rely on interleaved training (i.e., training on all to-be-

General Discussion

We have shown that a machine system can perform extrapolatory generalization through *predicate learning*. DORA used predicate learning to discover symbolic structure from training data without feedback, and without assuming any structured representations a priori. Crucially, the representations that DORA learned allowed it to extrapolate its knowledge to untrained situations. Specifically, the model was able to use the representations that it learned playing Breakout to successfully play a new game, Pong. Importantly, just as with human players, generalizing to a new game like Pong was fast (one-shot) and did not affect the system's ability to play a previously learned game. To our knowledge, we present the first demonstration of human-like generalization, or extrapolation, in a machine system that learns from experience, and which does not assume structured representations to begin with.

Humans radically outperform machines in numerous domains, particularly when making inferences. The power of human generalization appears to stem from our ability to use structured representations (e.g., Dumas & Hummel, 2005; Dumas, Hummel, & Sandhofer, 2008; Hummel & Holyoak, 1997, 2003; Lake et al., 2015, 2017; Martin & Dumas, 2017). The ability to discover structured representations from experience advances models of human cognition, exceeds the performance of current DNNs on video game transfer, and extends the principles of general machine learning by enabling extrapolatory generalization.

Of course, DORA still radically underperforms human behavior writ large (humans do much more than play a few video games). People have much richer mental representations, which they acquire from a wide range of experiences in a myriad of contexts over their lives. However, the fact that we could approximate human-like performance using only structured representations of relative dimensions, speaks to the power of these representations (cf. Biederman, 1987; Lake et al., 2017).

A predicate learning approach offers an account of how complex concepts might develop without the need to hardwire or encode the necessary information or structure into the system a priori. As such, we address limitations of current structure-based accounts of cognition (e.g., Kemp, 2015; Lake et al., 2015; Tenenbaum, Kemp, Griffiths, & Goodman, 2011), and offer a solution to the classic generalization problem that DNNs face (Bowers, 2017; Marcus, 2018a). The ability to learn predicates from experience, and to generalize those representations to new inputs and contexts, may have substantial impact on theories of human reasoning, language representation and processing (Martin, 2016; Martin & Dumas, 2017).

Though we do not assume innate representational types, we do not believe that the expressive power of our system negates the possibility that innate structures and biases exist in the human brain (Carey, 2009; Marcus, 2018b). Predicate learning makes a few clear claims about what infrastructure might be present in order to learn human-like structured representations. First, the system needs an innate or assumed ability to separate and compare streams of information (i.e., in banks of units connected to the same perceptual layer). Such a computational structure implies, for instance, a form of perceptual memory. Second, the system needs the capacity to learn to respond to temporal signals. In our network, this capacity is partially realized by layers of laterally inhibitive units. Beyond these computational primitives, other innate capacities or

learned tasks simultaneously). Block training, like we use (and which humans often engage in) still produces problems for DNNs.

knowledge may also exist (e.g., biases to attend to specific kinds of information), but we do not need to assume them in order to learn representations that support human-like extrapolatory generalization (cf. Marcus, Marbelstone, & Dean, 2014).

The mechanism we have identified can be extended to more complex structures and to generalization across a wider range of experiences. This extension is tractable in two ways: first, under predicate learning, additional training, especially across different contexts and datasets, will result in richer and richer representations which become more articulated and specified with experience. Second, predicate learning supports combining simple representations into more complex structures as needed. The ability to identify useful combinations of simpler relational concepts can bootstrap learning more complex concepts. For instance, a complex concept like *support* might be built out of simpler concepts (e.g., a *contact* point of the supporting object *lower* than the contact point of the supported object). By combining our approach with more sophisticated reinforcement and model selection algorithms (e.g., Kemp, 2012; Lake et al., 2015), we might find a strong way forward, with our system providing an account of where the structured representations that form the basis of more complex models come from in the first place.

Finally, we highlight the fact that predicate learning was able to discover structured representations from experience because it exploits temporal regularities in the data. We believe that this solution represents a fundamental formal and neurophysiological alignment between how human-like representations can be achieved in a system that learns, and how distributed neural computing systems, including cortical assemblies, process information (see Martin & Dumas, 2017 for a discussion; see also Hummel & Biederman, 1992; Hummel & Holyoak, 1997, 2003; and von der Malsburg, 1986 for a historical precedent). Neural oscillations, or brain rhythms, (Buzsáki, 2006) have long been implicated as indices of neural information processing (e.g., Gray, König, Engel, & Singer, 1989) in many systems, even when those systems differ in scale and configuration (Marder & Goaillard, 2006) and have changed the nature of theories of the neural implementation of human memory (Klimesch, 1999) and of cortical speech and language processing (Luo & Poeppel, 2007). Learning symbolic structure from signals that naturally occur in distributed computing systems like the brain offers a promising avenue of research whereby the computational principles that yield the highest forms of the human mind (e.g., relational reasoning, formal and natural language processing) can be realized in systems based on the computational primitives of neurophysiological systems. Being able to generalize in a human-like way, or extrapolate symbolic structure, while using representations learned from experience is, in our view, a defining feature of the human mind. By capturing this ability in a machine system, we have addressed a core function of human thinking.

REFERENCES

- Agrawal, R., Imieliński, T., & Swami, A. (1993). Mining association rules between sets of items in large databases. In *Acm sigmod record* (Vol. 22, No. 2, pp. 207-216). ACM.
- Biederman, I. (1987). Recognition-by-components: a theory of human image understanding. *Psychological review*, 94(2), 115.
- Bowers, J. S. (2017). Parallel Distributed Processing Theory in the Age of Deep Networks. *Trends in Cognitive Sciences*.
- Buzsáki, G. (2006). *Rhythms of the Brain*. Oxford University Press.
- Carey, S. (2009). *The origin of concepts*. Oxford University Press.

- Doumas, L. A., & Hummel, J. E. (2005). Approaches to modeling human mental representations: What works, what doesn't and why. *The Cambridge handbook of thinking and reasoning*, ed. KJ Holyoak & RG Morrison, 73-94.
- Doumas, L. A. A., Hummel, J. E., & Sandhofer, C. M. (2008). A theory of the discovery and predication of relational concepts. *Psychological Review*, 115(1), 1-43.
- Forbus, K. D., Ferguson, R. W., Lovett, A., & Gentner, D. (2017). Extending SME to Handle Large-Scale Cognitive Modeling. *Cognitive Science*, 41(5), 1152-1201.
- Furmanski, C. S., & Engel, S. A. (2000). An oblique effect in human primary visual cortex. *Nature Neuroscience*, 3(6), 535.
- Gentner, D. (2003). Why we're so smart. In D. Gentner and S. Goldin-Meadow (Eds.), *Language in mind: Advances in the study of language and thought*, 195-235. Cambridge, MA: MIT Press.
- Gray, C. M., König, P., Engel, A. K., & Singer, W. (1989). Oscillatory responses in cat visual cortex exhibit inter-columnar synchronization which reflects global stimulus properties. *Nature*, 338(6213), 334.
- Holyoak, K. J., & Hummel, J. E. (2000). The proper treatment of symbols in a connectionist architecture. *Cognitive dynamics: Conceptual change in humans and machines*, 229-263.
- Holyoak, K. J., & Thagard, P. (1996). *Mental leaps: Analogy in creative thought*. MIT press.
- Hummel, J. E., & Biederman, I. (1992). Dynamic binding in a neural network for shape recognition. *Psychological Review*, 99(3), 480.
- Hummel, J. E., & Holyoak, K. J. (1997). Distributed representations of structure: A theory of analogical access and mapping. *Psychological Review*, 104(3), 427.
- Hummel, J. E., & Holyoak, K. J. (2003). A symbolic-connectionist theory of relational inference and generalization. *Psychological Review*, 110(2), 220.
- Kemp, C. (2012). Exploring the conceptual universe. *Psychological Review*, 119(4), 685.
- Kirkpatrick, J., Pascanu, R., Rabinowitz, N., Veness, J., Desjardins, G., Rusu, A. A., ... & Hassabis, D. (2017). Overcoming catastrophic forgetting in neural networks. *Proceedings of the National Academy of Sciences*, 114(13), 3521-3526.
- Klimesch, W. (1999). EEG alpha and theta oscillations reflect cognitive and memory performance: a review and analysis. *Brain research reviews*, 29(2-3), 169-195.
- Lake, B. M., Salakhutdinov, R., & Tenenbaum, J. B. (2015). Human-level concept learning through probabilistic program induction. *Science*, 350(6266), 1332-1338.
- Lake, B. M., Ullman, T. D., Tenenbaum, J. B., & Gershman, S. J. (2017). Building machines that learn and think like people. *Behavioral and Brain Sciences*, 40.
- LeCun, Y., Bengio, Y., & Hinton, G. (2015). Deep learning. *Nature*, 521(7553), 436-444.
- Luo, H., & Poeppel, D. (2007). Phase patterns of neuronal responses reliably discriminate speech in human auditory cortex. *Neuron*, 54(6), 1001-1010.
- Marcus, G. F. (1998). Rethinking eliminative connectionism. *Cognitive Psychology*, 37(3), 243-282.
- Marcus, G. (2018a). Deep Learning: A Critical Appraisal. *arXiv preprint arXiv:1801.00631*.
- Marcus, G. (2018b). Innateness, AlphaZero, and Artificial Intelligence. *arXiv preprint arXiv:1801.05667*.
- Marcus, G., Marblestone, A., & Dean, T. (2014). The atoms of neural computation. *Science*, 346(6209), 551-552.
- Marder, E., & Goaillard, J. M. (2006). Variability, compensation and homeostasis in neuron and network function. *Nature Reviews Neuroscience*, 7(7), 563.
- Martin, A. E. (2016). Language processing as cue integration: Grounding the psychology of language in perception and neurophysiology. *Frontiers in Psychology*, 7.
- Martin, A. E., & Doumas, L. A. (2017). A mechanism for the cortical computation of hierarchical linguistic structure. *PLoS Biology*, 15(3), e2000663.

- Moore, C., & Engel, S. A. (2001). Neural response to perception of volume in the lateral occipital complex. *Neuron*, 29(1), 277-286.
- Mnih, V., Kavukcuoglu, K., Silver, D., Rusu, A. A., Veness, J., Bellemare, M. G., ... & Petersen, S. (2015). Human-level control through deep reinforcement learning. *Nature*, 518(7540), 529.
- Tenenbaum, J. B., Kemp, C., Griffiths, T. L., & Goodman, N. D. (2011). How to grow a mind: Statistics, structure, and abstraction. *Science*, 331(6022), 1279-1285.
- von der Malsburg, C. (1995). Binding in models of perception and brain function. *Current Opinion in Neurobiology*, 5(4), 520-526.
- von der Malsburg, C. (1986). Am I thinking assemblies? In *Brain theory* (pp. 161-176). Springer, Berlin, Heidelberg.

ACKNOWLEDGEMENTS

This research was supported by grant ES/K009095/1 from Economic and Social Research Council of the United Kingdom to AEM. We thank Mante S. Nieuwland and Hugh Rabagliati for comments on an earlier version of this work, and Dylan Opdam and Zina Al-Jibouri for assistance with the initial research. Source code is available from github.com/AlexDoumas/BrPong_18.

Human-like generalization in a machine through predicate learning — Supplemental material

S1: Details of DORA's Operation

DORA's front end consists of a simple neural network pre-processor trained for each game. The input consisted of the $210 \times 160 \times 3$ images generated by the gym environment. This input was flattened to a vector of size 100800. There were three fully-connected hidden relu layers. The output layer was a fully connected sigmoid layer of size $(210 + 160) \times \text{number of critical objects for the game}$. The produced the x, y coordinates of the topmost leftmost corner of the objects as well as their width and height, and their x and y velocity.

For each game, a dataset of 160000 labelled images were created using the pre-processors. Of these 120000 were used for training and 40000 for validation. The networks were trained with the ADAM algorithm with default parameters and binary cross entropy loss for 5 epochs. We obtained a validation loss of 0.003 for Breakout and Pong.

Because in Pong the left paddle is red, the ball is white, and the right paddle is green, object identification was based on colour. In particular the program applied a mask based on each colour and found the bounding rectangle of each object. The bounding rectangles contained the x, y coordinates along with the width and height. In Breakout the paddle and the ball are red, object identification was based on the position and shape of the objects. In particular, the program applied a red mask to the screen and then found the bounding rectangles of the paddle and the ball. In cases where the ball touched the paddle and a single bounding rectangle was obtained, the fixed y-axis of the paddle (189), the height of the paddle (4) and the width (2) and height (4) of the ball were used as points of reference to infer the x, y coordinates as well as the width and height of both objects. The same front end was used to train a deep recurrent neural network for comparison to DORA (see S4).

DORA's processing architecture begins with representations of objects coded as flat feature vectors (see Figure 3a). These representations are similar to representations in traditional connectionist architectures where elements are coded by distributed collections of units. For example, DORA might represent a toy ball with a node connected to a set of features (Figure S1a).³ In short, DORA begins with objects coded conjunctively by flat feature vectors. (In terms of cortical computation, feature nodes can be thought of as aggregate units, perceptual representations, or activation states over networks.)

³ While we use labels for semantic feature units, the specific content of the units coding for a property are unimportant to DORA (in fact, the model is actually unaware of the labels given to semantic units). So long as there is something common across the units representing a set of objects, DORA can learn an explicit representation of this commonality. That is, for the purposes of DORA's learning algorithm, all that matters is there is something invariant across instances of a *container* (which there must be for us to learn the concept), and that the perceptual system is capable of responding to this invariance (which, again, there must be for us to respond similarly across instances of containment in the world; for a more complete discussion of the role of invariance in perception see, e.g., Biederman, 1987).

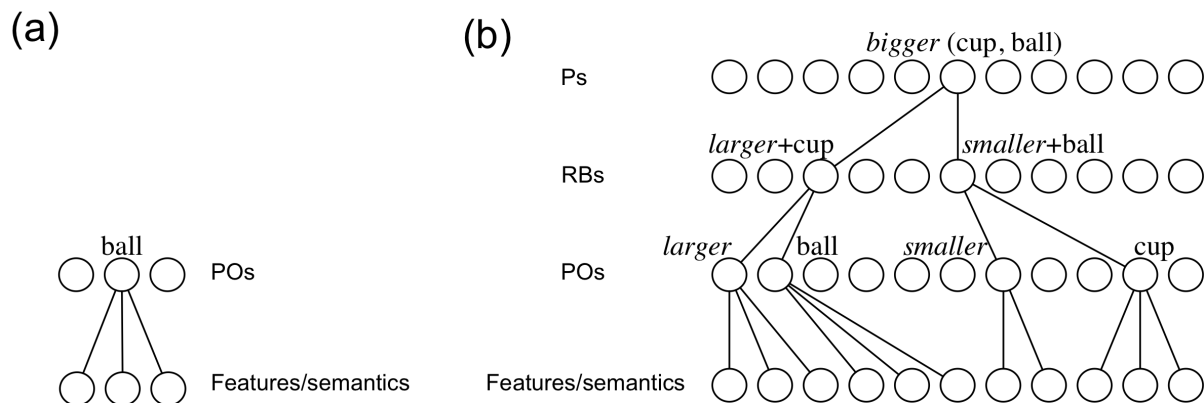


Fig. S1.

Representations in DORA. (a) DORA's starting state. DORA begins with representations of objects connected to lists of their features. (b) Representation of the proposition *bigger* (cup, ball) instantiated in layers of bidirectionally connected nodes. DORA learns propositional representations from examples of representations like those in (a).

DORA learns representations of a form we call LISAese (Figure S1b) via unsupervised learning (described in full below). Full propositions in LISAese are coded by layers of units in a connectionist computing framework (Figure S1b). At the bottom of the hierarchy, features (or semantic) nodes code for the featural properties of represented instances in a distributed manner. At the next layer, localist predicate and object units (POs) conjunctively code collections of semantic units into representations of objects and roles. At the next layer localist role-binding units (RBs) conjunctively bind object and role POs into linked role-filler pairs. Finally, proposition units (Ps) link RBs to form whole relational structures.

DORA's processing architecture is composed of four mutually exclusive banks of (Figure S2): the *focus of attention/driver*, the *active memory/recipients*, *long-term-memory* (LTM), and the *emerging-active-memory/emerging-recipient* (EM). Each set consists of a layered network coding for POs, RBs, and Ps (i.e., there are specific layers coding for POs, RBs, and Ps in the driver, and another set of layers coding for POs, RBs, and Ps in the recipient). Feature (or semantic) units are common across all networks (i.e., driver, recipient, LTM, and EM units are connected to the same pool of semantic units).

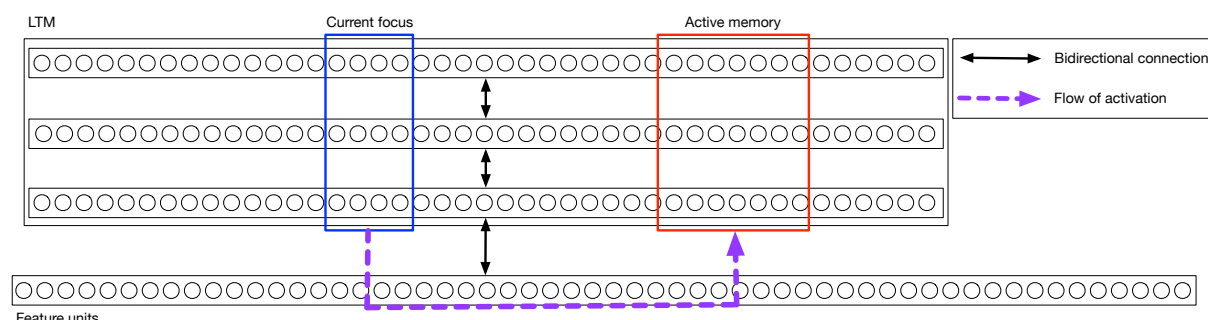


Fig. S2.

DORA's computational macrostructure.

An *analog* in DORA is a complete story, event, or situation. Analogs are represented by a collection of token (P, RB and PO) units that together represent the propositions in that analog. While token units are not duplicated within an analog (e.g., within an analog, each proposition that refers to Don connects to the same "Don" unit), separate analogs have non-identical token

units (e.g., Don will be represented by one PO unit in one analog and by a different PO in another analog). All analogs are connected to the same pool of semantic units. The semantic units thus represent general type information and token units represent instantiations of those things in specific analogs (Hummel & Holyoak, 1997, 2003). For example, if in some analog, the token (PO) unit “Fido” is connected to the semantics “animal”, “dog”, “furry” and “Fido”, then it is a token of an animal, a dog, a furry thing and of the particular dog Fido.

The driver controls the flow of activation in DORA. The driver corresponds to the DORA’s current focus of attention. Units in the driver pass activation to the semantic units. Because the semantic units are shared by propositions in all sets, activation flows from the driver to propositions in the other three sets. All of DORA’s operations (i.e., *retrieval*, *mapping*, *predicate learning*, *relation formation*, *schema induction*, and *generalisation*) proceed as a product of the units in the driver activating semantic units, which in turn activate units in the various other sets (as detailed below). During *retrieval*, patterns of activation generated on the semantic units by units in the driver, activate representations in LTM, which are retrieved into the recipient. Propositions in the recipient are available for *mapping* onto propositions in the driver. Active driver units activate corresponding (i.e., semantically similar) units in the recipient, allowing DORA to learn mapping connections between them. Mappings between units in the driver and recipient are the basis of DORA’s ability to *learn new predicate representations* and to *form higher arity structures* from lower arity structures. Finally, DORA can *learn schemas* from mapped propositions in the driver and recipient, which are encoded into the EM, and may subsequently be encoded into LTM and later enter the driver or recipient.

When a proposition enters the focus of attention, or in in working memory, role-filler bindings must be represented dynamically on the units that maintain role-filler independence (i.e., POs and semantic units; see Hummel & Holyoak, 1997). In DORA, roles are dynamically bound to their fillers by phase-lag, or by either systematic asynchrony or systematic synchrony of firing. During asynchrony-based—or phase-lag-1—binding, as a proposition in the driver becomes active, bound objects and roles fire in direct sequence, and out of synchrony with other bound role-filler sets. Binding information is carried in the proximity of firing (e.g., with roles firing directly before their fillers). During synchrony-based—or phase-lag-0—binding, as a proposition in the driver becomes active bound objects and roles fire together, and out of synchrony with other bound role-filler sets. Details of how time-based firing patterns are established and exploited are described below.

The model is based on a core set of neurocomputational computing principles. The model assumes (a) a layered architecture, with banks of layered units connected to a common pool of feature units. (b) Lateral inhibition between units in the layered banks. (c) Yoked inhibitors on units that accumulate input from their yoked units, and units at higher layers. (d) The capacity for Hebbian learning. There is ample evidence for all of these basic assumptions in the human neuroscience literature (e.g., Morrison et al., 2013).

In DORA firing is organized by the *phase set*, or the set of units in the driver that is currently active and firing out of phase. We take the driver to be the focus of DORA’s attention, or what DORA is currently “thinking about”. The general sequence of events in DORA’s operation is outlined below. The details of these steps, along with the relevant equations and parameter values, are provided in the subsections that follow. Importantly, DORA is very robust to the values of the parameters (see Doumas et al., 2008). Throughout the equations in this section, we will use the variable a to denote a unit’s activation, n its (net) input, and w_{ij} to denote the connection from unit i to unit j .

1. Visual pre-processing
2. Bring an analog into the driver, D , (selected at random).
3. Initialize the activations of all units in the network to 0.
4. Select the firing order, C , of propositions in D to become active. (In all the simulations described here, firing order is random. However, see Hummel & Holyoak, 2003, for a detailed description of how a system like DORA can set its own firing order according to the constraints of pragmatic centrality and text coherence.)
5. Run SRM.
 - 5.1. Do basic similarity calculation.
 - 5.2. Do basic relative magnitude calculation.
6. Run phase set operations. Repeat the following until each RB in D has fired three times if mapping, or once, otherwise:
 - 6.1. If there are RB units in C that have not fired during the current phase set (i.e., are not inhibited, see text below), randomly select an uninhibited RB, RB_C , in C . Otherwise, if there are PO units in P that have not fired during the current phase set (i.e., are not inhibited, see text below), randomly select an uninhibited PO unit, PO_C , in C . (As noted above, in all the simulations described here, firing order is random. However, see Hummel & Holyoak, 2003, for a detailed description of how a system like DORA can set its own firing order according to the constraints of pragmatic centrality and text coherence.)
 - 6.2. Update the network in discrete time steps until the global inhibitor fires. On each time step t do:
 - 6.2.1. Set input to RB_C or PO_C to 1.
 - 6.2.2. Update modes of all P units in the recipient set, R . (We do not use higher-order relations in any of the simulations described herein so the mode of P units is always at 1, however, we include this step for completeness.)
 - 6.2.3. Update inputs to all token units in driver.
 - 6.2.4. Update input to the PO inhibitors.
 - 6.2.5. Update input to the RB inhibitors.
 - 6.2.6. Update the local inhibitor.
 - 6.2.7. Update the global inhibitor.
 - 6.2.8. Update input to semantic units.
 - 6.2.9. Update input to all token units in the recipient, R , and the emerging recipient, N .
 - 6.2.10. Update activations of all units in the network.
 - 6.2.11. Update all mapping hypotheses (if mapping).
 - 6.2.12. Run retrieval (if performing retrieval).
 - 6.2.13. Run comparison-based unsupervised learning (if learning).
 - 6.2.13.1. If there are no active RB units in P , then run comparison-based predication.
 - 6.2.13.2. If there are active RB units in P , then run refinement learning:
 - 6.2.13.2.1. Run relational generalization.
 - 6.2.13.2.2. Run relation formation.
 - 6.2.13.2.3. Run predicate refinement.
7. Update mapping connections (if applicable).
8. Store results of learning (if any).

Step 5.1: Do basic similarity calculation

Similarity calculation is performed when two PO units are compared and co-activated across the driver and recipient. During comparison, the activation of the compared POs is set to 1, and

they pass activation to their constituent semantic units (see description of 6.2.8 below). This process continues for 25 iterations. Subsequently, similarity is calculated by the equation:

$$sim_{ij} = \frac{1}{1 + \sum_i (1 - s_i)} , \quad (S1)$$

where, sim_{ij} is the 0 to 1 normalised similarity of PO unit i and PO unit j , and s_i is the activation of semantic unit i .

Step 5.2: Do basic relative magnitude calculation

Magnitude calculation is performed when two POs from the same analog that both code some dimension are present in the driver. First, the activation of the two POs is set to 1, and they pass activation to the semantics coding the dimension they have in common (e.g., height), and any invariant SRM units (i.e., the semantics coding “same”, “different”, “more”, and “less”; initially POs are not connected to any of these semantics) to which they are connected. Input and activation of the semantic units is updated for 25 iterations (see steps 6.2.8 and 6.2.10, respectively).

If no SRM unit is active above threshold ($=.7$), then the activation of the active magnitude semantics is clamped at 1, and the compared PO units compete to respond to the pattern of activation on the semantic units, otherwise, skip to *Step 4* (see below). Until the compared PO activation settles—remaining unchanged for 4 iterations—the network is updated in discrete time steps. On each time step, the input and activation of compared POs is updated. During magnitude calculation PO units are receiving input only from semantic units. Consequently, input to PO unit i is calculated using the equation,

$$n_i = \frac{\sum_j a_j w_{ij}}{1 + num(j)} , \quad (S2)$$

where j are semantic units connected to i , w_{ij} is the weight between units i and j , and $num(j)$ is the number of semantic units j . PO units update their activation by the leaky integrator function:

$$\Delta a_i = \gamma n_i (1.1 - a_i) - \delta a_i]_1^0 , \quad (S3)$$

where Δa_i is the change in activation of unit i , a_i is the activation of unit i , γ ($=0.3$) is a growth parameter, n_i is the net input to unit i , and δ ($=0.1$) is a decay parameter.

Upon settling, the network is updated in discrete time steps until the local inhibitor fires. On each time step, the local inhibitor is updated (see step 6.2.6), the input and activation of compared PO units is updated (by Eqs. S2 and S3, respectively), and active POs learn connections to semantic units by the equation:

$$\Delta w_{ij} = a_i (a_j - w_{ij}) , \quad (S4)$$

where, w_{ij} is the weight between PO unit i and semantic unit j , a_j is the activation of semantic unit j , a_i is the activation of PO unit i . Connection weights between POs and semantic units are limited to values between 0 and 1. If, upon settling, both compared POs are active, the “same” semantic unit becomes active until the local inhibitor fires. Otherwise, if, upon settling, only one compared PO is active, the “more” semantic unit becomes active and the network is updated in discrete time steps (as above) until the local inhibitor fires. After the local inhibitor fires, the “less” semantic unit becomes active and the network is updated in discrete time steps (as above) until the local inhibitor fires.

If any SRM units are active above threshold (≈ 0.7), these units compete via lateral inhibition, with the “more” semantic inhibiting “less” and “same”, and the “same” semantic inhibiting “more” and “less” (see section S2 for how this circuit is learned). After the SRM units settle, activation of the most active SRM unit is clamped to 1, and the network is updated in discrete time steps (as above) until the local inhibitor fires. If the “more” semantic unit was previously active, the “less” semantic unit becomes active and is clamped to 1. Again, the network is updated in discrete time steps (as in *Step 3*) until the local inhibitor fires.

During relative magnitude calculation, additional invariant patterns emerge. The relative magnitude calculation procedure described above also provides information about the relative differences of the relative differences in magnitude—or, second-order relative magnitude information (e.g., the distance between A and B is greater than the distance between C and D). More specifically, by consequence of the comparison procedure, items that are more different will take less time to settle than items that are less different, and items that are entirely similar will take less time to settle than items that are almost entirely similar. The network can exploit these invariance responses—in much the same way it exploits the different patterns of settling when items of different and similar magnitude are compared—to detect relative differences in the relative differences of magnitudes. That is, the system can detect (and then respond to) second order relative magnitude information with the same process that it uses to detect and respond simple relative magnitude information.

When two POs coding for some magnitude are compared as described directly above, second-order magnitude difference (i.e., the magnitude of the magnitude difference) can be approximated by the equation:

$$D_D = f_a(t_s) , \quad (S5)$$

where, D_D is the second-order magnitude difference, f_a is a function, and t_s is a measure of the time to settling during the comparison process. For present purposes, t_s is a count of the number of iterations that the relative magnitude calculation required to settle.

The function f_a maps a value of t_s to a second-order magnitude difference, D_D . Any number of functions, f_a , will produce reasonable results, including a simple linear function. We do not claim to have an optimised f_a at present, but for present purposes we define the function as:

$$f_a(x) = \ln(x) , \quad (S6)$$

where, \ln is the natural logarithm.

The same relative magnitude calculation procedure that produces responses to analog magnitudes also responds to values of D_D in precisely the same manner. As such, the same

magnitude calculation method will produce implicit invariant responses to second-order magnitude differences, and explicit predicate representations of these responses can be learned as described in the main text and below.

Step 6.2.2. Update mode of all P units in the recipient set

P units in all propositions operate in one of three modes: Parent, child, and neutral, as described by Hummel and Holyoak (1997, 2003). The idea of units firing in “modes” may sound “non-neural”, but Hummel, Burns & Holyoak (1994) describe how it can be accomplished with two or more auxiliary nodes with multiplicative synapses. A P unit in parent mode is operating as the linking element of a multi-place relational proposition. Parent P units excite and are excited by RBs to which they are downwardly connected (i.e., RB units that they link into multi-place relational propositions). In child mode, a P unit is acting as the argument of a higher-order proposition. Child P units excite and are excited only by RBs to which they are upwardly connected. In neutral mode, P units take input from all RBs to which they are upwardly and downwardly connected. The mode of P units in the driver are set at the beginning of each run by the rule given in the order of operations outline above. Each P unit i in R updates its mode, m_i , according to:

$$m_i = \begin{cases} Parent(1), & RB_{above} < RB_{below} \\ Child(-1), & RB_{above} > RB_{below} , \\ Neutral(0), & otherwise \end{cases} \quad (S7)$$

where RB_{above} is the summed input from all RB units to which i is upwardly connected (i.e., relative to which, i serves as an argument) and RB_{below} is the summed input from all RB units to which it is downwardly connected.

Steps 6.2.3. Updating input to all token units in the driver

P units Each P unit i in D in parent mode updates its input as:

$$n_i = \sum_j a_j - \sum_k a_k , \quad (S8)$$

where j are all RB units below P unit i to which i is connected and k are all other P units in D that are currently in parent mode. P units in D in child mode update their inputs by:

$$n_i = \sum_j a_j - \sum_k a_k - s \sum_l a_l - s \sum_m 3a_m , \quad (S9)$$

where j are RB units to which i is upwardly connected, k are other P units in the driver that are currently in child mode, l are all PO units in the driver that are not connected to the same RB as i , and m are all PO units that are connected to the same RB (or RBs) as i . When DORA is

operating in binding-by-asynchrony mode, $s = 1$; when it is operating in binding-by-synchrony mode (i.e., like LISA), $s = 0$.

RB units RB units in the driver update their inputs by:

$$n_i = \sum_j a_j + \sum_k a_k - s \sum_l 3a_l - 10I_i, \quad (\text{S10})$$

where j are all P units in parent mode to which RB unit i is upwardly connected, k are all PO units connected to i , l are all other RB units in D , and I_i is the activation of the RB inhibitor yoked to i .

PO units PO units in the driver update their input by:

$$n_i = \sum_j a_j G - \sum_k a_k - s \sum_l a_l - s \sum_m 3a_m - 10I_i, \quad (\text{S11})$$

where j are all RB units to which PO unit i is connected, G is a gain parameter attached to the weight between the RB and its POs (POs learned via DORA's comparison based predication algorithm—and thus with mode=1; see section 6.2.13.1 below—have $G=2$ and 1 otherwise), k are P units in D that are currently in child mode and not connected to the same RB as i , l are all PO units in the driver that are not connected to the same RB as i , m are PO units that are connected to the same RB (or RBs) as i , and I_i is the activation of the PO inhibitor yoked to i . When DORA is operating in binding-by-asynchrony mode, $s = 1$; when it is operating in binding-by-synchrony mode (i.e., like LISA), $s = 0$.

Steps 6.2.4 and 6.2.5. Update input to the PO and RB inhibitors

Every RB and PO unit is yoked to an inhibitor unit i . Both RB and PO inhibitors integrate input over time as:

$$n_i^{(t+1)} = n_i^{(t)} + \sum_j a_j w_{ij}, \quad (\text{S12})$$

where t refers to the current iteration, j is the RB or PO unit yoked to inhibitor unit i , and w_{ij} is the weight between RB or PO inhibitor i and its yoked RB or PO unit (set to 1). Inhibitor units become active ($a_i = 1$) when n_i is greater than the activation threshold ($=220$). RB inhibitors are yoked only to their corresponding RB. PO inhibitors are yoked both to their corresponding PO and all RB units in the same analog. As a result, at any given instant, PO inhibitors receive twice as much input as RB inhibitors, and reach their activation threshold twice as fast. POs, therefore, oscillate twice as fast as RBs. PO and RB inhibitors establish the time-sharing that carries role-filler binding information and allows DORA to dynamically bind roles to fillers. All PO and RB inhibitors become refreshed ($a_i = 0$ and $n_i = 0$) when the global inhibitor (Γ_G ; described below) fires.

Steps 6.2.6 and 6.2.7. Update the local and global inhibitors

The local and global inhibitors, Γ_L and Γ_G respectively (see e.g., Horn and Usher, 1990; Horn et al., 1992; Usher and Nieber, 1996; von der Malsburg and Buhman, 1992), serve to allow units in the recipient to keep pace with firing of units in the driver. The local inhibitor is inhibited to inactivity ($\Gamma_L = 0$) by any PO in the driver with activation above $\Theta_L (= 0.5)$, and becomes active ($\Gamma_L = 10$) when no PO in the driver has an activity above Θ_L . During asynchronous binding, the predicate and object POs time-share. There is a period during the firing of each role-filler pair after the one PO fires and before the other PO becomes active when no PO in the driver is very active. During this time the local inhibitor becomes active and inhibits all PO units in the recipient to inactivity. Effectively, Γ_L serves as a local refresh signal, punctuating the change from predicate to object or object to predicate firing in the driver, and allowing the units in the recipient to keep pace with units in the driver.

The global inhibitor works similarly. It is inhibited to inactivity ($\Gamma_G = 0$) by any RB in the driver with activation above $\Theta_G (= 0.5)$ and becomes active ($\Gamma_G = 10$) when no RB in the driver is active above threshold. During the transition between RBs in the driver there is a brief period when no driver RB are active above Θ_G . During this time Γ_G inhibits all units in the recipient to inactivity, allowing units in the recipient to keep pace with units in the driver.

Step 6.2.8. Update input to semantic units

Semantic units update their input as:

$$n_i = \sum_{j \in S \in (D, R)} a_j w_{ij} , \quad (S13)$$

where j is all PO units in S , which is the set of propositions in the driver, D , and recipient R , and w_{ij} is the weight between PO unit j and semantic unit i .

Step 6.2.9. Update input to token units in the recipient and the emerging recipient

Input to all token units in the recipient and emergent recipient are not updated for the first 5 iterations after the global or local inhibitor fires. This delay in update occurs in order to allow units in the recipient and emergent recipient to respond to the pattern of activation imposed on the semantic units by the driver PO unit that wins the competition to become active after an inhibitor fires.

P units P units in parent mode in the recipient update their inputs by:

$$n_i = \sum_j a_j + M_i - \sum_k 3a_k - \Gamma_G , \quad (S14)$$

where j are all RB units to which P unit i is downwardly connected, k are all other P units in the recipient currently in parent mode and M_i is the mapping input to i :

$$M_i = \sum_j a_j (3w_{ij} - \text{Max}(\text{Map}(i)) - \text{Max}(\text{Map}(j))), \quad (\text{S15})$$

where j are token units of the same type as i in the driver (e.g., if i is a RB unit, j is all RB units in the driver), $\text{Max}(\text{Map}(i))$ is the highest of all unit i 's mapping connections, and $\text{Max}(\text{Map}(j))$ is the highest of all unit j 's mapping connections. As a result of Eq. S15, an active token unit in the driver will excite any recipient unit to which it maps and inhibit all recipient units of the same type to which it does not map.

P units in child mode in the recipient update their inputs by:

$$n_i = \sum_j a_j + M_i - \sum_k a_k - \sum_l a_l - \sum_m 3a_m - \Gamma_G, \quad (\text{S16})$$

where j are all RB units to which i is upwardly connected, M_i is the mapping input to i , k are all other P units in the recipient currently in child mode, l are POs in the recipient that are not connected to the same RB (or RBs if i is connected to multiple RBs) as i , and m are PO units connected to the same RB (or RBs) as i .

RB units RB units in the recipient update their input by:

$$n_i = \sum_j a_j + \sum_k a_k - \sum_l a_l + M_i - \sum_m 3a_m - \Gamma_G, \quad (\text{S17})$$

where j are P units currently in parent to which RB unit i is upwardly connected, k are P units currently in child mode to which i is downwardly connected, l are PO units to which unit i is connected, M_i is the mapping input to i , and m are other RB units in the recipient.

PO units PO units in the recipient update their input by:

$$n_i = \sum_j a_j + SEM_i + M_i - \sum_k a_k - \sum_l a_l - s \sum_m 3a_m - \sum_n a_n - \Gamma_G - \Gamma_L, \quad (\text{S18})$$

where j is RB units to which PO unit i is connected (input from j is only included on phase sets beyond the first), SEM_i is the semantic input to unit i , M_i is the mapping input to unit i , k is all PO units in the recipient that are not connected to the same RB (or RBs if unit i is connected to multiple RBs) as i , l is all other P units in the recipient currently in child mode that are not connected to the same RB (or RBs) as i , m is PO units connected to the same RB (or RBs) as i , and n is RB units in the recipient to which unit i is not connected. When DORA is operating in binding-by-asynchrony mode, $s = 1$; when it is operating in binding-by-synchrony mode (i.e., like LISA), $s = 0$. SEM_i , the semantic input to i , is calculated as:

$$SEM_i = \frac{\sum_j a_j w_{ij}}{1 + num(j)} , \quad (S19)$$

where j are semantic units, w_{ij} is the weight between semantic unit j and PO unit i , and $num(j)$ is the total number of semantic units i is connected to with a weight above $\theta (=0.1)$. Semantic input to POs is normalized by a Weber fraction so that the PO unit that best matches the current pattern of semantic activation takes the most semantic input, and semantic input is not biased by the raw number of semantic features that any given PO is connected to (see Hummel & Holyoak, 1997, 2003; Marshall, 1995).

Step 6.2.10. Update activations of all units in the network

All token units in DORA update their activation by Eq. S3. As noted above, semantic unit activations are divisively normalized, and semantic units update their activation by the equation:

$$a_i = \frac{n_i}{\max(n_i)} , \quad (S20)$$

where a_i is the activation of semantic unit i , n_i is the net input to semantic unit i , and $\max(n_i)$ is the maximum input to any semantic unit. There is physiological evidence for divisive normalization in the feline visual system (e.g., Albrecht & Geisler, 1991; Bonds, 1989; Heeger, 1992) and psychophysical evidence for divisive normalization in human vision (e.g., Foley, 1994; Thomas & Olzak, 1997).

RB and PO inhibitors, i , update their activations according to a threshold function:

$$a_i = \begin{cases} 1, & n_i > \Theta_{IN} \\ 0, & otherwise \end{cases} , \quad (S21)$$

where $\Theta_{IN} = 220$.

Step 6.2.11. Update all mapping hypotheses

DORA's mapping algorithm is adopted from Hummel and Holyoak (1997, 2003). During the mapping process, DORA learns mapping hypotheses between all token units in the driver and token units of the same type in the recipient (i.e., between P units, between RB units and between PO units in the same mode [described below]). Mapping hypotheses initialize to zero at the beginning of a phase set. The mapping hypothesis between an active driver unit and a recipient unit of the same type is updated by the equation:

$$\Delta h_{ij}^t = a_i^t a_j^t \quad (S22)$$

where a_i^t is the activation of driver unit i at time t , and a_j^t is the activation of recipient unit j at time t .

Step 6.2.12 Run retrieval

DORA uses a variant of the retrieval routine described by Hummel and Holyoak (1997). During retrieval propositions in the driver fire as described above for one phase set. Units in the dormant/LTM set become active in response to the patterns of activation imposed on the semantics by active driver POs. After RBs in the driver have fired once, DORA retrieves propositions from LTM probabilistically using the Luce choice axiom:

$$L_i = \frac{R_i}{\sum_j R_j} \quad (S23)$$

where L_i is the probability that P unit i will be retrieved into working memory, R_i is the maximum activation P unit i reached while during the retrieval phase set and j are all other P units in LTM. If a P unit is retrieved from LTM, the entire structure of tokens (i.e., RBs, POs, and P units that serve as arguments of the retrieved P unit) are retrieved into working memory.

Step 6.2.13. Run comparison-based unsupervised learning

DORA's comparison-based learning routines are unsupervised. In the current version of the model, learning is licensed whenever 70% of the driver token units map to recipient items (this 70% criterion is arbitrary, and in practice 100% of the units nearly always map). If learning is licensed DORA runs unsupervised learning. If the driver contains single objects, not yet bound to any predicates (i.e., each RB in the driver is bound only to a single PO), then DORA runs comparison-based predication learning. Otherwise, DORA runs refinement learning.

Step 6.2.13.1. Comparison-based predication

As detailed in the text, during comparison-based predication (CBP) for each PO in the driver that is currently active, and maps to a unit in the recipient with a mapping connection above the threshold Θ_{MAP} ($=0.5$), DORA recruits a new PO unit (i.e., a PO connected to no semantic features) in the recipient. The mode of the existing PO units in both the driver and recipient is set to 0 and the mode of the newly inferred PO is set to 1. The mode of PO units is used to distinguish POs acting as objects from POs acting as predicates (i.e., those POs learned via comparison-based learning). Learned predicate POs have a higher gain on their connection weights to RBs than do object POs (see section 6.2.3 above). This gain allows predicates to fire before objects during asynchronous binding and reflects our assumptions that humans favour things they learn when making inferences (see, e.g., Goldstone et al., 1991). The mode of POs is also important for assuring mappings from predicates to other predicates and from objects and other objects when DORA uses LISA-like synchrony binding (i.e., when roles and their fillers fire in synchrony). Although we do not use synchrony-based binding for the reported simulations, we mention it here and implement it in our code for the purposes of completeness. DORA learns connections between the new PO and all active semantics by the equation:

$$\Delta w_{ij} = a_i(a_j - w_{ij})\gamma \quad (S24)$$

where Δw_{ij} is the change in weight between the new PO unit, i , and semantic unit, j , a_i and a_j are the activations of i and j , respectively, and γ is a growth rate parameter. By Eq. S24, the weight between the recruited PO and a semantic unit will asymptote to that semantic unit's activation. During CBP, DORA also infers a new RB unit in the recipient. The activation of

each inferred unit is set to 1 and remains at 1 until Γ_G or Γ_L fires. DORA learns a connection with a weight of 1 between corresponding active token units (i.e., between P and RB units. and between RB and PO units) that are not already connected.

Step 6.3.13.2. Refinement Learning

Step 6.2.13.2.1: Relational generalisation. Relational generalisation is the process by which relational inferences are made in DORA. The relational generalisation algorithm is a self-supervised learning algorithm adopted from that used in Hummel and Holyoak's (2003) LISA model. During self-supervised learning, if no token units are active in the recipient to match active token units in the driver, DORA will activate token units in the recipient that match active token units in the driver. As detailed in Eq. S15, when a token unit j in the driver is active, it will produce a global inhibitory signal to all recipient units to which it does not map. A uniform inhibition in the recipient signals DORA to activate a unit of the same type (i.e., P, RB, PO) in the recipient as the active token unit in the driver. DORA learns connections between corresponding active tokens in the emerging recipient (i.e., between P and RB units. and between RB and PO units) by the simple Hebbian learning rule in Eq. S4 (where unit j is the newly active token unit, and unit i is the other active token unit). Connections between PO units and semantic units are updated by Eq. S24.

Step 6.2.13.2.2: Relation formation. As described in the main text, when DORA successfully maps sets of role-filler bindings in the driver to sets of role-filler bindings in the recipient, the resulting pattern of firing on the recipient RB units is exactly like what would emerge from RB units joined by a common P unit (i.e., mapped RBs in the recipient fire out of synchrony but in close temporal proximity, and within each mapped RB, mapped POs fire out of synchrony but in close temporal proximity). During relation formation DORA exploits this temporal pattern to link the recipient RBs (along with their respective POs) into a full proposition—i.e., a multi-place relation. This process is accomplished as a case of SSL. When an RB in the recipient becomes active, if no P units are active in the recipient, then a P unit is recruited in the recipient via SSL. The newly recruited P unit remains active (activation=1) until the end of the phase set and learns connections to active RBs by Eq. S4 (where unit j is the newly active P unit, and unit i is the active RB unit). When the phase set ends, connection weights between the new P unit i and any RBs to which it has connections, j , are updated by the equation:

$$w_{ij} = \begin{cases} 1, & w_{ij} > 0 \text{ and } \sum_k w_{ik} \geq 2 \\ 0, & \text{otherwise} \end{cases}, \quad (\text{S25})$$

where w_{ij} is the connection weight between P unit i and RB unit j , and w_{ik} is the connection weight between i , and RB unit k where k is all RB units (including j) in the recipient. Essentially, if the new P has at least two connections to RB units (and so sum over k of w_{ik} is greater than or equal 2), then DORA retains the connections between the recruited P and all RBs to which it has learned connections; if the sum is less than two, then it discards the connections (along with the P unit). This convention ensures that DORA does not learn superfluous P units (i.e., Ps that connect only to a single RB). The exact same result is accomplished by learning connections between P and RB units by Hebbian learning, and then truncating all connections if the sum of connections to the newly recruited P unit is not greater than 1.

Step 6.3.13.2.3: Predicate refinement. As detailed in the text, during predicate refinement DORA learns a refined representation of mapped propositions or role-filler sets. For each PO in the driver that is currently active, and maps to a unit in the recipient with a mapping connection above the threshold $\Theta_{\text{MAP}} (=0.7)$, DORA infers a PO unit connected to no semantic features in the emerging recipient with a mapping connection to the active driver unit. DORA learns connections between the new PO and all active semantics by Eq. S24. DORA also licenses self-supervised learning (SSL). During SSL, DORA infers token units in the emerging recipient that match active tokens in D (the driver). Specifically, DORA infers a structure unit in the emerging recipient in response to any unmapped token unit in D . If unit j in D maps to nothing in the emerging recipient, then when j fires, it will send a global inhibitory signal to all units in the emerging recipient (Eq. S15). This uniform inhibition, unaccompanied by any excitation in the recipient us a signal that DORA exploits, and infers a unit of the same type (i.e., P, RB, PO) in the emerging recipient. Inferred PO units in the emerging recipient have the same mode as the active PO in the driver. The activation of each inferred unit in the emerging recipient is set to 1. DORA learns connections between corresponding active tokens in the emerging recipient (i.e., between P and RB units. and between RB and PO units) by Eq. S4 (where unit j is the newly inferred token unit, and unit i is any other active token unit). To keep DORA's representations manageable (and decrease the runtime of the simulations), at the end of the phase set, we discard any connections between semantic units and POs whose weights are less than 0.1.

Step 7. Update mapping connections

Mapping connections are updated at the end of each phase set. First, all mapping hypotheses are normalized by the equation:

$$h_{ij} = \left(\frac{h_{ij}}{\text{MAX}(h_i, h_j)} \right) - \text{MAX}(h_{kl}) \quad (\text{S26})$$

where, h_{ij} is the mapping hypothesis between units i and j , $\text{MAX}(h_i, h_j)$ is the largest hypothesis involving either unit i or unit j , and $\text{MAX}(h_{kl})$ is the largest mapping hypothesis where either $k=i$ and $l \neq j$, or $l=j$ and $k \neq i$. That is, each mapping hypothesis is normalised divisively: Each mapping hypothesis, h_{ij} between units i and j , is divided by the largest hypothesis involving either unit i or j . Next each mapping hypothesis is normalized subtractively: The value of the largest hypothesis involving either i or j (not including h_{ij} itself) is subtracted from h_{ij} . The divisive normalization keeps the mapping hypotheses bounded between zero and one, and the subtractive normalization implements the one-to-one mapping constraint by forcing mapping hypotheses involving the same i or j to compete with one another (see Hummel & Holyoak, 1997). Finally, the mapping weights between each unit in the driver and the token units in the recipient of the same type are updated by the equation:

$$\Delta w_{ij} = \eta(1.1 - w_{ij})h_{ij}^0_1 \quad (\text{S27})$$

where Δw_{ij} is the change in the mapping connection weight between driver unit i and recipient unit j , h_{ij} is the mapping hypothesis between unit i and unit j , η is a growth parameter, and Δw_{ij} is truncated for values below 0 and above 1. After each phase set, mapping hypotheses are reset to 0. The mapping process continues for three phase sets.

S2: Learning a neural circuit coding invariant similarity and relative magnitude responses

As noted in the main text, there are several ways to instantiate a neural response to the invariant signal produced during similarity and magnitude comparison. Here we present one solution, but—also as noted in the main text—we make no strong theoretical claims about the veracity of any particular instantiation. Rather, our claim is that the neural system learns to respond to the invariant pattern of firing that occurs when similar and different magnitudes are compared and uses this response as the basis for learning invariant semantic features that support implicit similarity and relative magnitude (SRM) processing, which can serve as the basis for learning structured (i.e., predicate) representations.

Figure S3 depicts the magnitude response network. The network instantiates the magnitude comparison operation described in section S1 and behaves equivalently to that description. This network is based on classical connectionist computing principle and is learnable via unsupervised learning. In the following we first describe the behavior of the network, then a basic algorithm for learning this network.

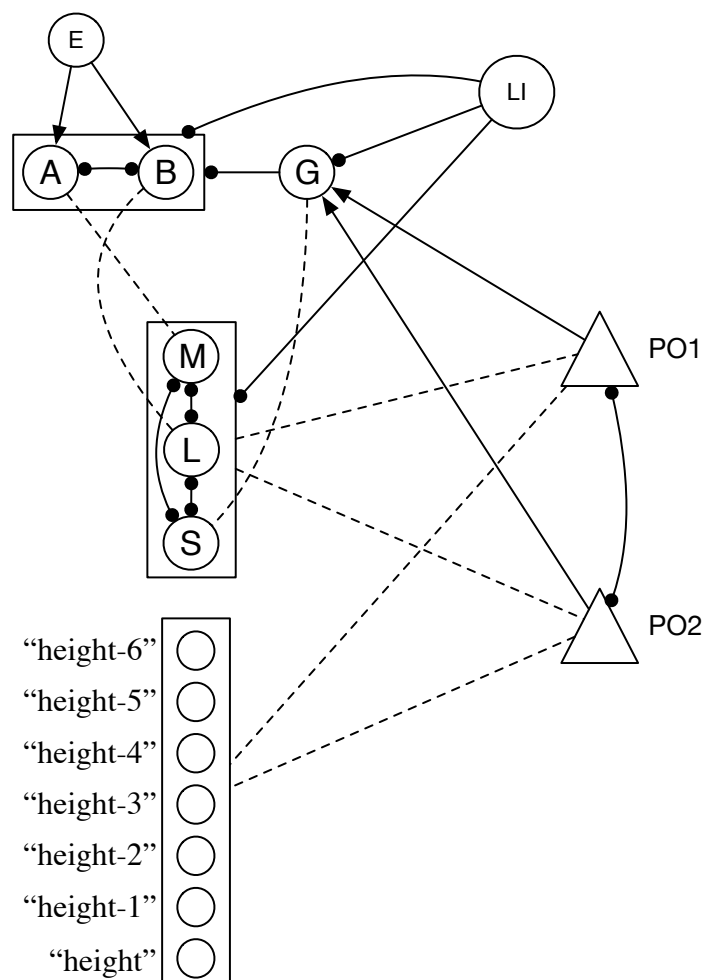


Fig. S3.

A network that responds to the invariant patterns of firing that occur during magnitude comparison. Node (A) marks early in comparison process. Node (B) marks later in the comparison process. Node (G) is a gating unit that fires only when receiving input from multiple units, and marks two active POs. Node (E) fires once the activation of the PO units (triangles) has settled (see main text and Appendix A). Node (M) comes to stand as the invariant of ‘more’; node (L) comes to stand as the invariant of

‘less’; node (S) comes to stand as the invariant of ‘same’. LI=local inhibitor. Solid lines with circles at either endpoint specify two-way inhibitory connections. Solid lines with a circle at only one endpoint specify one-way inhibitory connections where the node at the circle end is inhibited. Solid lines with arrows at one endpoint specify one-way excitatory connections where the node at the arrow end is excited. Dashed lines indicate excitatory connections between modified via unsupervised Hebbian learning, as described in the text. Where nodes are contained in a box, connections to and from that box apply to all units in that box.

During magnitude comparison, PO units (nodes labelled PO1 and PO2 in Fig. S3) compete to become active. PO units are connected to semantic units indicating their absolute magnitude, with greater magnitudes encoded by larger numbers of units (see above). As a consequence, when the two PO units code different absolute magnitudes, the PO unit connected to the greater magnitude will win the completion to become active and inhibit the PO unit connected to the lesser magnitude.

When the units settle, node E in Fig. S3 fires. As can be seen in Fig. S3, node E passes activation to nodes A and B. Node A is randomly more strongly connected to E and becomes active more quickly, inhibiting node B to inactivity. Node A also activates to the “more” semantic, and the active PO unit learns a connection to the “more” semantic (see main text). When the inhibitor on the active PO fires, the active PO unit is inhibited to inactivity, and the local inhibitor (LI) fires (see section S3). The LI inhibits unit A, allowing node B to become active as the next PO unit also becomes active. Node B inhibits node A and passes activation to the “less” semantic. The active PO unit learns a connection to the “less” semantic.

When both PO units code for the same semantic, they settle into a stable state of mutual activation. Two active PO units will activate gating node G. Node G inhibits nodes A and B and passes activation the “same” semantic. The active PO units learn connections to the “same” semantic.

The magnitude circuit consists of nodes A, B, G, and the magnitude semantics. This circuit is learned via an unsupervised learning algorithm. Nodes A, B, and G follow the activation function:

$$a_i = \begin{cases} 1 & n_i > \theta_i \\ 0, & \text{otherwise} \end{cases} , \quad (\text{S28})$$

where a_i is the activation of threshold unit i , n_i is the input to unit i , and θ_i is the threshold of unit i . The input to unit i is calculated by:

$$n_i = \sum_j a_j w_{ij} - \rho_i , \quad (\text{S29})$$

where, n_i is the input to unit i , a_j is the activation of unit j connected to unit i , w_{ij} is the connection weight between units i and j , and ρ_i is the refraction of unit i . Node G is a gating unit (i.e., it has a threshold greater than 1). Refractions for A and B units have a base level, θ_b , and are adjusted as a function of time since last firing by:

$$\rho_i = \frac{10}{1 + e^{x-\vartheta}} , \quad (\text{S30})$$

where, x is the number of iterations since unit i has fired, and ϑ is the threshold of PO inhibitors (=110). Connection weights between units A and B and unit E, and connection weights between units A, B, G

and semantics are initially set to a random value between 0 and 1. PO units and semantic units behave as described in section S1.

During learning, connection weights between units A, B, G and semantic units are adjusted through Eq. S4. Learning begins 3 iterations after POs settle. In short, after learning, the unit most strongly connected to unit E will become the A unit, and the unit with the next strongest connection to E will become the B unit. Similarly, the semantic unit that ends up the most strongly connected to A becomes the semantic invariant for “more”, the semantic unit that ends up the most strongly connected to B becomes the semantic invariant for “less”, and the semantic unit that ends up the most strongly connected to G becomes the semantic invariant for “same”. Connections between semantic units and active PO units are updated by Eq. S4.

S3 Details of gameplay simulations.

Several agents were created and trained to play break out and pong as implemented in the OpenAI Gym environment (Brockman et al., 2016).

Deep-Q-network

A Deep Q-Network (DQN; Mnih et al., 2015) was trained to play Breakout and Pong. The raw 210×160 frames produced by the AIGym environment were pre-processed by first converting their RGB representation to grey-scale and down-sampling it to a 105×80 image. We stacked the last 4 consecutive frames to form the input each state.

The input to the neural network was the $105 \times 80 \times 4$ pre-processed state. The first hidden convolutional layer applied 16 filters of size 8×8 with stride 4 with a relu activation function. The second hidden convolutional layer applied 32 filters of size 4×4 with stride 2 with a relu activation function. The third hidden layer was fully connected of size 256 with a relu activation function. The output layer was fully connected with size 6 and a linear activation function.

We implemented all the procedures of Mnih et al. (2015) to improve training stability, in particular: (a) We used memory replay of size 1,000,000. (b) We used a target network which was updated every 10,000 learning iterations. (c) We fixed all positive rewards to be 1 and all negative rewards to be -1 , leaving 0 rewards unchanged. (d) We clipped the error term for the update through the Huber loss.

Deep neural network

We trained a deep neural network (DNN) in a supervised manner to play Breakout and Pong and tested generalization between games. The network was trained using random frame skipping.

We used the same preprocessors described previously to get the x and y coordinates of the ball and the paddles in Breakout and Pong. In both cases a pre-processed frame corresponded to a vector of size 6, where the first two units corresponded to the x and y position of the center of the left paddle in Pong and were left as zero for Breakout. The third and fourth units coded the position of the ball and the fifth and sixth units coded the position of the agent-controlled paddle for both games.

The input to the neural network was a vector of size 24 corresponding to the pre-processed last seen 4 frames. This was fed to three fully connected layers of size 100 each with a relu activation function. The output layer was fully connected with size 6 and a linear activation function.

The criteria for training was the correct action to take in order to keep the agent-controlled paddle aligned with the ball. In Breakout if the ball was to the left of the paddle the correct action was 'LEFT', if the ball was to the right of the paddle the correct action was 'RIGHT' and if the ball and the paddle were at the same level on the x-axis the correct action was 'NOOP'. In Pong if the ball was higher than paddle the correct action was 'RIGHT', if the ball was lower than paddle the correct action was 'LEFT' and if the ball and the paddle were at the same level

on the y-axis the correct action was ‘NOOP’. This action was encoded as a one-hot vector (i.e., activation of 1 for the correct action and zero for all other actions).

We implemented a replay memory of maximum size one million. At each training iteration the model received a frame, added it to its state representation of 4 frames and choose an action. Then, the model saved its current state to the replay memory, sampled a batch of 32 states and performed 1 step of gradient descend. The replay memory was initialized with five thousand states from a random policy. We trained the model for four million iterations.

DORA

We used DORA to simulate learning structured representations from screen shots from the game Breakout. This simulation aims to mirror what happens when a child (or adult) learns from experience without a teacher or guide.

We started with screenshots from Breakout, experienced during 250 games with random move selection. When learning in the world, objects have several extraneous properties. To mirror this point, each pre-processed image was also attached to a set of 10 additional features selected randomly from a set of 1000 features. These additional features were included to act as noise, and to make learning more realistic. (Without these noise features, DORA learned exactly as described below, only more quickly.)

DORA attempted to learn from these basic representations in an unsupervised manner. On each learning trial, DORA selected one pair of objects from the current screenshot at random. DORA attempted to characterize any relations that existed between the objects using any relations it has previously learned (initially, it had learned nothing, and so nothing was returned). DORA selected a dimension at random and ran the two objects through the SRN circuit over that dimension. If the semantics returned matched anything in LTM (e.g., “more” and “less” “x-position”), then DORA used that representation from LTM to characterize the current objects. DORA then ran (or attempted to run) its retrieval, mapping, SDM comparison, predication, multi-place relation learning, and refinement routines (see section S1), and stored the representations that it learned in LTM. We placed one constraint on DORA’s retrieval algorithm such that more recently learned items were favoured for retrieval. Specifically, with probability .6, DORA attempted to retrieve from the last 100 analogs that it had learned. This constraint followed our assumption that items learned more recently are more salient and more likely to be available for retrieval.

We defined a relational selectivity metric, S_i , for unit i as:

$$S_i = \frac{MEAN(w_{ij})}{1 + MEAN(w_{ik})}, \quad (S31)$$

where w_{ij} are the weights of the connections between unit i and all relevant features j (i.e., those defining a specific magnitude or similarity relation or role of a said relation), and w_{ik} are the weights of the connections between unit i and all other semantic features, j . One was added to the denominator to normalize the quality measure to between 0 and 1. A higher quality denoted stronger connections to the semantics defining a specific relation relative to all other connections (i.e., a more pristine representation of the relation). Figure S4 shows the relational quality of the representations in DORA’s LTM after each 100 learning trials for the first 2500

learning trials (roughly all the learning trials from the first 250 games of Breakout; where a learning trial is defined as above).

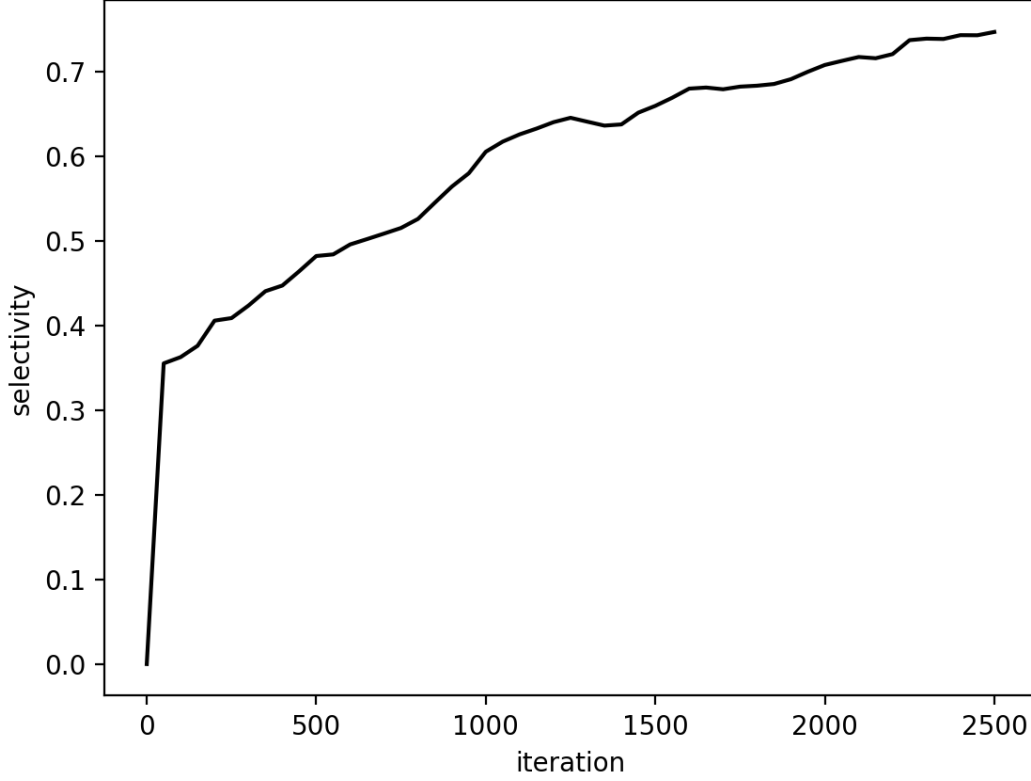


Fig. S4.
Results of DORA’s learning from Breakout screenshots.

These results clearly demonstrate that DORA learns structured representations of similarity and relative magnitude relations from unstructured (i.e., flat feature vector) representations of objects that include only absolute values on dimensions and extraneous noise features. Figure S5 shows the number of representations of simple objects, single-place predicates, and multi-place relations in DORA’s LTM after each 100 learning trials. During learning, DORA initially learned simple single-place predicate representations encoding absolute values on dimensions. DORA then used these representations for SRM computation, refined these representations, and linked mapped sets of single-place predicates to form whole multi-place relational structures, which it then further refined through additional comparisons. Through comparison-based learning, DORA acquired representations of whole relational structures encoding relative magnitudes on all the encoded dimensions. DORA learned representations of *higher* (where one predicate PO was connected most strongly to the semantics ‘more’ & ‘y’, the other connected to ‘less’ & ‘y’), *more-x* (where one predicate PO was connected most strongly to ‘more’ & ‘x’, and the other ‘less’ & ‘x’), *later* (where one predicate PO was connected most strongly to ‘more’ & ‘time’, and the other ‘less’ & ‘time’), *same-height* (where both predicate POs were connected most strongly to ‘same’ & ‘y’), *same-x* (where both predicate POs were connected most strongly to ‘same’ & ‘x’), and *same-time* (where both predicate POs were connected most strongly to ‘same’ & ‘time’). Moreover, DORA also learned representations of *greater* (x,y) and *same* (x,y) that were independent of any particular dimensions. That is, DORA learned relations that coded strongly for only the invariant features of *more* & *less* and

same, that were otherwise not strongly connected to any other semantic features (Phenomenon 5). These representations developed after DORA had learned some dimension specific magnitude relations (e.g., *bigger* and *wider*), and compared these representations and learned from the results. This result mirrors the development of abstract magnitude development in children (e.g., Sophian, 2017). The results indicate that DORA can learn structured representations of relative magnitude relations from object encodings that include only absolute values on dimensions and noise.

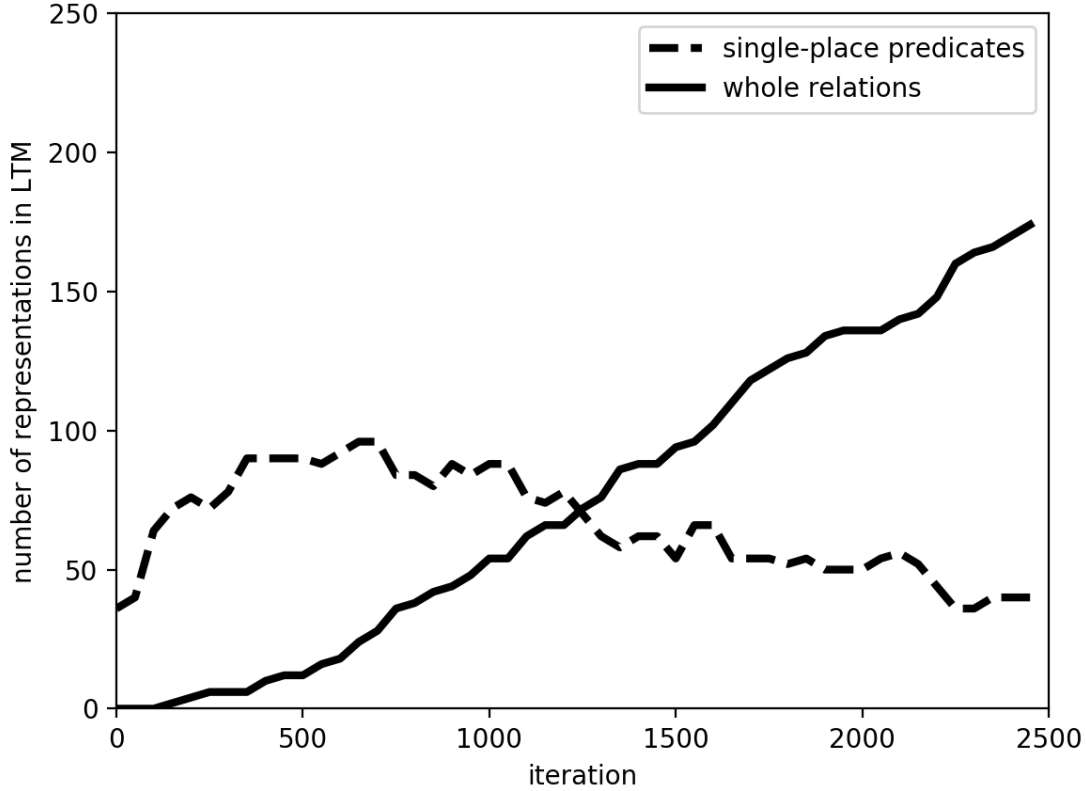


Fig. S5.

The number of representations of simple objects, single-place predicates, and whole relations in DORA's LTM after each 100 learning trails.

For the supervised learning structure, two lookup tables were generated. The first lookup table was one dimensional and consisted of the possible dimensions. The values in this table represented the learning values which were initialized at 0 and updated during training. The second lookup table was a four dimensional table, with the possible dimensions along the first axis, on the second axis the three possible predicates (i.e., *same*(ball, paddle), *more*(ball, paddle), *more*(paddle, ball)), on the third axis, the possible trajectories of the ball and the paddle (*same* (ball1, ball2), *more* (ball1, ball2), *more* (ball2, ball1), *same* (paddle1, paddle2), *more* (paddle1, paddle1), *more* (paddle2, paddle1)), and on the fourth axis the possible actions that DORA can take (left, right, do nothing). The values in this table were also initialized at 0 and updated during training.

By selecting the dimension with the highest value in the first table, a dimension x or y is chosen. This was done by first selecting the column corresponding to the current game state and then

selecting the dimension with the highest value in this column. In case of equal values, the first element in the column is taken.

Based on this chosen dimension, DORA attempted to characterize the relationship between the ball and the paddle on that dimension based on the predicates it had learned previously (see S3). To decide which of these predicates to apply, the coordinates on the chosen dimension are entered in DORA's entropy magnitude function. This function determines if the coordinates are equal, or which one is larger than the other.

Using the second lookup table, an action is chosen based on the generated predicate and chosen dimension. This is done by selecting the highest value within the column corresponding to this predicate and dimension. Applying an ϵ -greedy strategy, a random action can be chosen instead of the action taken from the table. ϵ is initialized at value 1.0 and decreased to 0.1 over the course of a 100 frames, where it remains for the remaining duration of the training process.

After the chosen action is performed in the environment, feedback is returned. If the action generated by DORA is equal to the action generated by the label, this reward will be 1. In any other case, the reward equals -1. In this manner, DORA will attempt to imitate the expert system that generates the labels. The values of both lookup tables are updated using Bellman equations [Mnih et al., 2015].

To generalise between games, DORA uses mapping and relational generalisation (section S1). Broadly, DORA uses the relational rule for move selection it has learned previously, maps this representation to the move selection for Pong, and then generalises a rule for move selection in Pong using relational generalisation. First, the representation of the moves available to DORA (sampled randomly during the first exposure to Pong) were placed in the driver. The rules learned during game play—represented using the relational representations DORA had learned during relation learning—were placed in the recipient. DORA attempted to map the representations in the driver to those in the recipient, and then used relational generalisation to infer rules for move selections based on the mappings it discover.

For example, the moves *moreY* (paddle, paddle2), *moreY* (paddle2, paddle), *sameY* (paddle, paddle2)—i.e., the moves available in the game of Pong—would be placed in the driver. During reinforcement learning, DORA learned that relations between the ball and paddle and the trajectory of the ball predicted proper move selection. Specifically, DORA learned that the state *moreX* (ball, paddle) with ball in state *moreX* (ball2, ball1) (i.e., the ball was currently at a position of further along that x-axis than it had been in the previous screen) predicted moving right, i.e., *moreX* (paddle2, paddle), that the state *moreX* (paddle, ball) and *moreX* (ball1, ball2) predicted moving left, i.e., *moreX* (paddle, paddle2), and that the state *sameX* (ball, paddle) predicted making no move, i.e., *sameX* (paddle, paddle2). These representations were placed in the recipient. DORA then attempted to map the representations in the driver to those in the recipient. Because of the shared relational and object similarity, *moreY* (paddle, paddle2) in the driver mapped to *moreX* (paddle, paddle2) in the recipient, *moreY* (paddle2, paddle) in the driver mapped to *moreX* (paddle2, paddle) in the recipient, and *sameY* (paddle, paddle2) in the driver mapped to *sameX* (paddle, paddle2) in the recipient. Through relational generalisation, DORA then filled in the missing rule information for the Pong game states.

More precisely, after mapping, DORA placed a representation of a rule in the driver, and the mapped move from Pong in the recipient. For example, DORA might place the rule *moreX* (ball, paddle) & *moreX* (ball2, ball1), then move = right, i.e., *moreX* (paddle2, paddle) in the

driver, and the mapped *moreY* (paddle, paddle2) in the recipient (Figure S6A). During mapping, DORA mapped the representations *moreX*(paddle2, paddle1) to *moreY* (paddle2, paddle1), reflecting the discovery of the correspondence between the move set in Breakout and in Pong (Figure S6B; mappings depicted as green double-headed lines). The relational generalisation algorithm is a self-supervised learning algorithm (see Doumas et al., 2008; Hummel & Holyoak, 2003). During self-supervised learning, if no token units are active in the recipient to match active token units in the driver, DORA will activate token units in the recipient that match active token units in the driver. As detailed in Eq. A15, when a token unit j in the driver is active, it will produce a global inhibitory signal to all recipient units to which it does not map. A uniform inhibition in the recipient signals DORA to activate a unit of the same type (i.e., P, RB, PO) in the recipient as the active token unit in the driver. Therefore, as the representation of *moreX* (ball, paddle) becomes active in the driver (Figure S6C), the units for *moreX* and *lessX* and paddle, all map to items in the recipient, while the units for ball and the *moreX*+ball, *lessX*+paddle, and the relation *moreX* (ball, paddle) map to nothing in the recipient. In response to this signal, DORA recruits nodes in the recipient with no strong connections to match the active and unmapped P, RB, and PO units in the driver (Figure S6D). These units then learn connections via Hebbian learning (Figure S6E). The same process will occur as the representation of *moreX* (ball2, ball1) becomes active in the driver (S6F-H). Through relational generalization, DORA matches the relational pattern of the driver rule with the available units in the recipient. The result is a representation of structurally similar rule: *moreY* (ball, paddle) & *moreY* (ball2, ball1), move = up, i.e., *moreY* (paddle2, paddle) (Figure 6I). This process was repeated for the other learned rules.

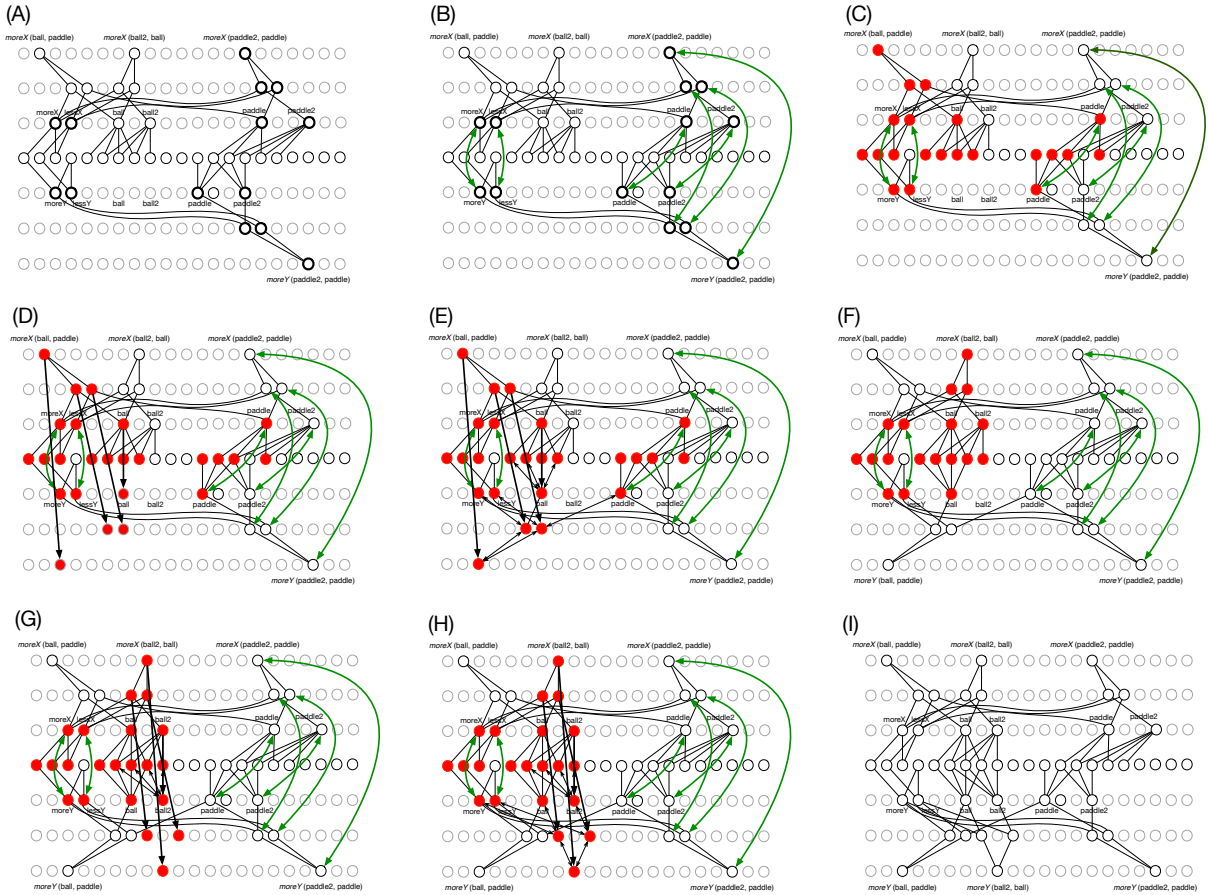


Fig S6.

Graphical depiction of relational generalisation in DORA. (A-B) a representation of the rule *moreX* (ball, paddle) & *moreX* (ball2, ball1), move = up, i.e., *moreX* (paddle2, paddle) is placed

in the driver, and mapped to the representation of *moreY* (paddle2, paddle1) in the recipient (green double arrowed lines). (C) The representation of *moreX* (ball, paddle) becomes active in the driver, and some active units have nothing to map to in the recipient. (D) DORA recruits and activates units to match the unmapped driver units, and learns connections between active token units in the recipient (open arrowed lines). The result is a representation of *moreY* (ball, paddle) in the recipient. (E-G) The same process occurs when *moreX* (paddle2, paddle1) becomes active in the driver. (I) The end result is a representation of the rule: *moreY* (ball, paddle) & *moreY* (ball2, ball1), move = up, i.e., *moreY* (paddle2, paddle).

Results

The main results appear in Fig. 3 in the main text. Figure S7 shows the learning trajectories of the various networks as a running average of 25 games. All networks learned to play Breakout well (Fig. 3a). Only humans and DORA generalized to playing Pong (Fig. 3b). After the DNN and DQN were trained on Pong, they were unsuccessful when returning to playing Breakout (Fig. 3c). By contrast, humans and DORA returned to playing Breakout with little difficulty (Fig. 3c). The results for all networks with starting with training on Pong, and then generalizing to Breakout were identical to starting with Breakout and generalizing to Pong.

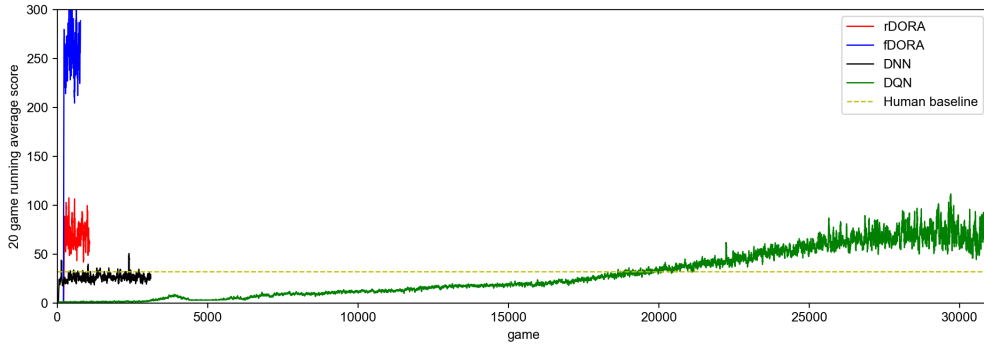


Fig. S7.

Scores of the various networks as a function of games played during learning. Calculated as a running average of 25 games.

Additional tests of the symbolic adequacy of the learned representations

The representations that DORA learns should behave like structured relational representations. That is, the representations DORA learns must meet the requirements of human relational representations. While almost any structured representations will support analogical mapping some more substantive hallmarks of relational representations (see Holyoak, 2012) are that they, (i) form the basis for solving cross mappings; (ii) support mapping similar, but non-identical predicates; (iii) support mapping objects with no featural overlap, including completely novel objects, if they play similar roles; and (iv) form the basis of overcoming the n-ary restriction.

During a cross-mapping, an object (object1) is mapped to a featurally less similar object (object2) rather than a featurally more similar object (object3) because it (object1) plays the same role as the less similar object (object2). For example, if cat1 chases mouse1 and mouse2 chases cat2, then the structural analogical mapping places cat1 into correspondence with mouse2 because both play the *chaser* role. The ability to find such a mapping is a key property of genuinely relational (i.e., as opposed to feature-based) processing (see, e.g., Gentner, 2003;

Holyoak, 2012; Penn et al., 2008). Cross-mappings serve as a stringent test of the structure sensitivity of a representation as they require violating featural or statistical similarity.

We tested the relations that DORA had learned in the previous part of this simulation for their ability to support cross-mappings. We selected two of the refined relations that DORA had learned previously at random, such that both selected representations coded for the same relation (e.g., both coded for *taller*, or both coded for *same-width*). We bound the relations to new objects, creating two new propositions, P1 and P2 such that the agent of P1 was semantically identical to the patient of P2 and patient of P1 was semantically identical to the agent of P2. For example, P1 might be *taller* (square, circle) and P2 might be *taller* (circle, square). DORA then attempted to map P1 onto P2. We were interested in whether DORA would map the square in P1 onto the circle in P2 (the correct relational mapping) or simply map the square to the square and the circle to the circle. We repeated this procedure 10 times (each time with a different randomly-chosen pair of relations). In each simulation, DORA successfully mapped the square in P1 to the circle in P2 and vice-versa (because of their bindings to mapped relational roles). DORA’s success indicates that the relations it learned in the first part of this simulation satisfy the requirement of supporting cross-mapping. DORA successfully solves cross-mappings because the correspondences that emerge between matching predicates and their corresponding RBs, during asynchronous binding force relationally similar objects into correspondence. For example, consider a case when DORA attempts to map *taller* (square, circle) in the driver, and *taller* (circle, square) in the recipient. When the *more-height*+square role-binding becomes active in the driver, because of asynchronous binding, the units coding for *more-height* will become active first, followed by the units coding for square. When *more-height* is active in the driver, it will activate *more-height* and its corresponding RB, *more-height*+circle, in the recipient. When the units coding for square subsequently become active in the driver, the active *more-height*+circle RB unit in the recipient (already in correspondence with the active *more-height*+square RB unit in the driver) will activate the square unit, thus putting circle and square into correspondence, and allowing DORA to map them.

We then tested whether the relations that DORA had learned would support mapping to similar but non-identical relations (such as mapping *taller* to *greater-than*) and would support mapping objects with no semantic over-lap, including novel objects, that play similar roles. Humans successfully map such relations (e.g., Bassok & Olseth, 1995; Gick & Holyoak, 1980, 1983; Kubose, Holyoak, & Hummel, 2002), an ability that Hummel and Holyoak (1997, 2003) have argued depends on the semantic-richness of our relational representations. We selected two of the refined relations that DORA had learned during the previous part of this simulation, R1 and R2 (e.g., *taller*(*x*,*y*) or *wider*(*x*,*y*)). Crucially, R1 and R2 both coded for SRM across different dimensions (e.g., if R1 coded *taller*, then R2 coded *wider*). Thus, each role in R1 shared 50% of its semantics with a corresponding role in R2 (e.g., the role *more-height* has 50% of its semantics in common with the role *more-width*). To assure that no mappings would be based on object similarity, none of the objects that served as arguments of the relations had any semantic overlap at all. To ensure that the mapping would work with completely novel objects, we created objects composed from semantic units that we added to DORA solely for these simulations (i.e., these were semantic units DORA had not “experienced” previously). We repeated this process 10 times, each time with a different pair of relations from DORA’s LTM. Each time, DORA mapped the agent role of R1 to the agent role of R2 and the patient role of R1 to the patient role of R2, and, despite their lack of semantic overlap, corresponding objects always mapped to one another (because of their bindings to mapped roles).

Finally, we tested whether the representations that DORA had learned would support violating the *n*-ary restriction: the restriction that an *n*-place predicate may not map to an *m*-place predicate when $n \neq m$. Almost all models of structured cognition follow the *n*-ary restriction (namely, those that represent propositions using traditional propositional notation and its isomorphs; see Doumas & Hummel, 2005). However, this limitation does not appear to apply to human reasoning, as evidenced by our ability to easily find correspondences between, say, *bigger* (Sam, Larry) on the one hand and *small* (Joyce) or *big* (Susan), on the other (Hummel & Holyoak, 1997).

To test DORA's ability to violate the *n*-ary restriction, we randomly selected a refined relation, R1, that DORA had learned in the previous part of this simulation. We then created a single place predicate (r2) that shared 50% of its semantics with the agent role of R1 and none of its semantics with the patient role. The objects bound to the agent and patient role of R1 each shared 50% of their semantics with the object bound to r2. DORA attempted to map R1 to r2. We repeated this process 10 times, each time with a different relation from DORA's LTM, and each time DORA successfully mapped the agent role of R1 to r2, along with their arguments. We then repeated the simulation such that r2 shared half its semantic content with the patient (rather than agent) role of R1. In 10 additional simulations, DORA successfully mapped the patient role of R1 to r2 (along with their arguments). In short, in all our simulations DORA overcame the *n*-ary restriction, mapping the single-place predicate r2 onto the most similar relational role of the multi-place relation R1.

Finally, as noted above, DORA also learned representations of *greater* (x,y) and *same* (x,y) that were independent of any particular dimensions (i.e., relations that coded strongly for only the invariant features of *more* & *less* and *same*, that were otherwise not strongly connected to any other semantic features). Importantly, these representations also met all the requirements of structured relational representations. We ran the exact same tests for cross-mapping, mapping arguments with no semantic overlap based on shared roles, and violating the *n*-ary restriction that are described above, but using the representations of abstract magnitude (i.e., *greater* (x,y)) that DORA had learned during training. Just as with DORA's dimensional SRM representations, DORA's more abstract SRM representations successfully performed a cross-mapping in 10 out of 10 simulations, mapped arguments with no semantic overlap based only on shared roles in 10 out of 10 simulations and overcame the *n*-ary restriction in 10 out of 10 simulations.

Additional references

- Albrecht, D. G., & Geisler, W. S. (1991). Motion selectivity and the contrast-response function of simple cells in the visual cortex. *Visual neuroscience*, 7(6), 531-546.
- Bassok, M., & Olseth, K. L. (1995). Judging a book by its cover: Interpretative effects of content on problem-solving transfer. *Memory & Cognition*, 23(3), 354-367.
- Bonds, A. B. (1989). Role of inhibition in the specification of orientation selectivity of cells in the cat striate cortex. *Visual neuroscience*, 2(1), 41-55.
- Brockman et al., 2016] Brockman, G., Cheung, V., Pettersson, L., Schneider, J., Schulman, J., Tang, J., and Zaremba, W. (2016). Openai gym. *arXiv preprint arXiv:1606.01540*.
- Foley, J. M. (1994). Human luminance pattern-vision mechanisms: masking experiments require a new model. *JOSA A*, 11(6), 1710-1719.
- Gick, M. L., & Holyoak, K. J. (1980). Analogical problem solving. *Cognitive psychology*, 12(3), 306-355.
- Gick, M. L., & Holyoak, K. J. (1983). Schema induction and analogical transfer. *Cognitive psychology*, 15(1), 1-38.
- Goldstone, R. L., Medin, D. L., & Gentner, D. (1991). Relational similarity and the nonindependence of features in similarity judgments. *Cognitive psychology*, 23(2), 222-262.

- Heeger, D. J. (1992). Normalization of cell responses in cat striate cortex. *Visual neuroscience*, 9(2), 181-197.
- Holyoak, K. J. (2012). Analogy and relational reasoning. *The Oxford handbook of thinking and reasoning*, 234-259.
- Kellman, P. J., Burke, T., & Hummel, J. E. (1999, August). Modeling perceptual learning of abstract invariants. In *Proceedings of the Twenty First Annual Conference of the Cognitive Science Society* (pp. 264-269).
- Kubose, T. T., Holyoak, K. J., & Hummel, J. E. (2002). The role of textual coherence in incremental analogical mapping. *Journal of memory and language*, 47(3), 407-435.
- Morrison, R. G., & Knowlton, B. J. (2012). Neurocognitive methods in higher cognition. *The Oxford Handbook of Thinking and Reasoning*, 67.
- Penn, D. C., Holyoak, K. J., & Povinelli, D. J. (2008). Darwin's mistake: Explaining the discontinuity between human and nonhuman minds. *Behavioral and Brain Sciences*, 31(2), 109-130.
- Sophian, C. (2017). *The origins of mathematical knowledge in childhood*. Routledge.
- Thomas, J. P., & Olzak, L. A. (1997). Contrast gain control and fine spatial discriminations. *JOSA A*, 14(9), 2392-2405.